PROGRESS IN UNDERSTANDING THE IMPACTS OF 3-D CLOUD STRUCTURE ON MODIS CLOUD PROPERTY RETRIEVALS FOR MARINE BOUNDARY LAYER CLOUDS

MODIS Science Team Meeting,
Silver Spring, June 2016

Zhibo Zhang
Physics Department/JCET, UMBC

Frank Werner (UMBC), Daniel Miller (UMBC), Steven Platnick (GSFC),
Andrew Ackerman (GISS),Larry Di Girolamo (UIUC), Kerry Meyer (GSFC),
Alexander Marshak (GSFC), Gala Wind (GSFC), Guangyu Zhao (UIUC)

Bi-spectral method for *simultaneous* retrieval of cloud optical thickness (COT) and effective radius (CER)

Bi-spectral
VNIR (e.g., 0.64, 0.86μm) band reflectance increases with COT, given a CER
SWIR (e.g., 2.1, 3.7μm) band reflectance decreases with CER, given a COT

Nakajima and King 1990 JAS

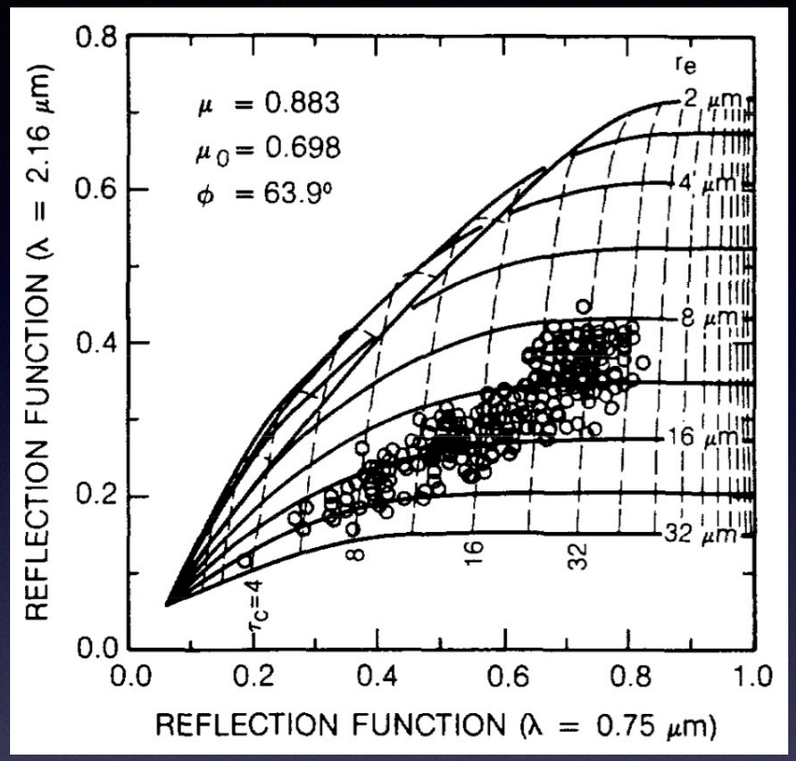

Widely Used
AVHRR, VIIRS
MODIS, SEVIRI, FY,
eMAS, MASTER
Suomi-NPP,GOES-R, …

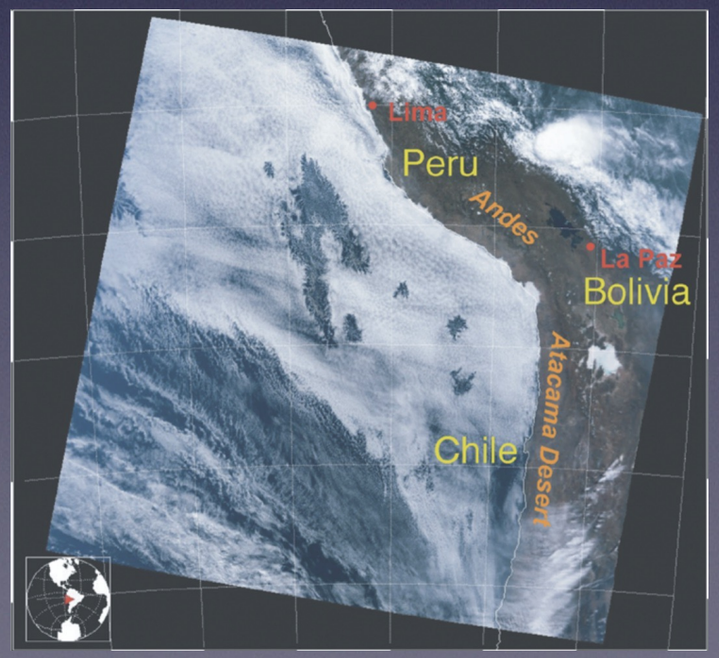

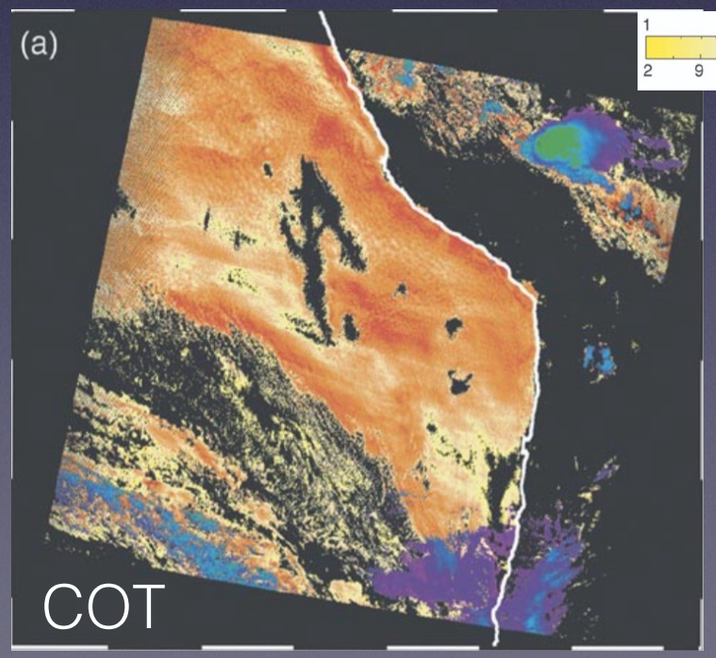

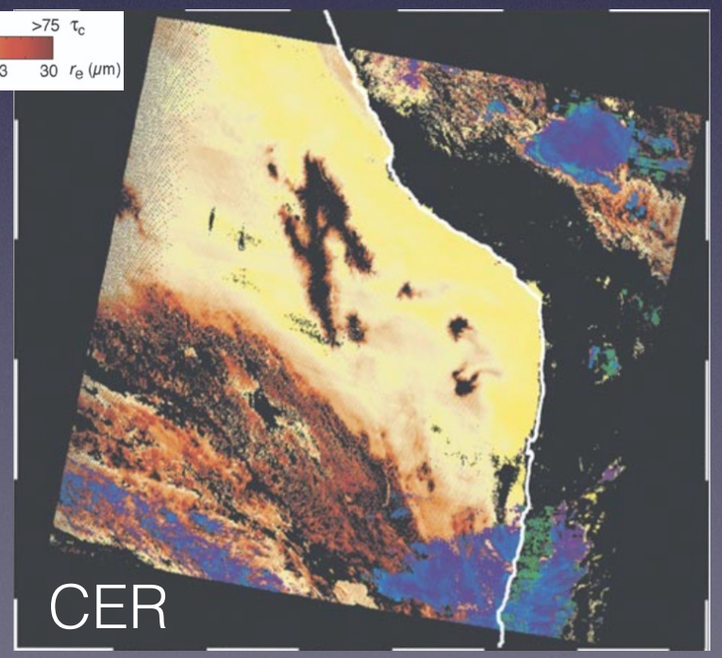

Platnick et al. 2003 IEEE TGRS

Key assumptions made in the *operational* MODIS cloud retrieval

- Within a pixel, cloud is both vertically and horizontally homogenous ("homogeneous pixel")
- A pixel is independent of surrounding pixels, i.e., no net horizontal photon transport ("independent pixel assumption—IPA")
- Cloud particle size distributions follow certain analytical functions, e.g., gamma or log-normal

What happens if a pixel is not homogeneous?

Outline

- Theory:
  - A novel framework based on 2-D Tayler expansion for quantifying the uncertainty in MODIS retrievals caused by sub-pixel reflectance inhomogeneity. (*Zhang et al. 2016)*
  - How cloud vertical structure influences MODIS LWP retrievals. (*Miller et al. 2016)*
- Observation:
  - Analysis of *failed* MODIS cloud property retrievals. *(Cho et al. 2015)*
  - Cloud property retrievals from 15m resolution ASTER observations. *(Werner et al. 2016)*
- Modeling:
  - LES-Satellite observation simulator *(Zhang et al. 2012, Miller et al. 2016)*.

Theoretical advances I:

A novel framework for quantifying the impact of Sub-pixel inhomogeneity on MODIS retrievals

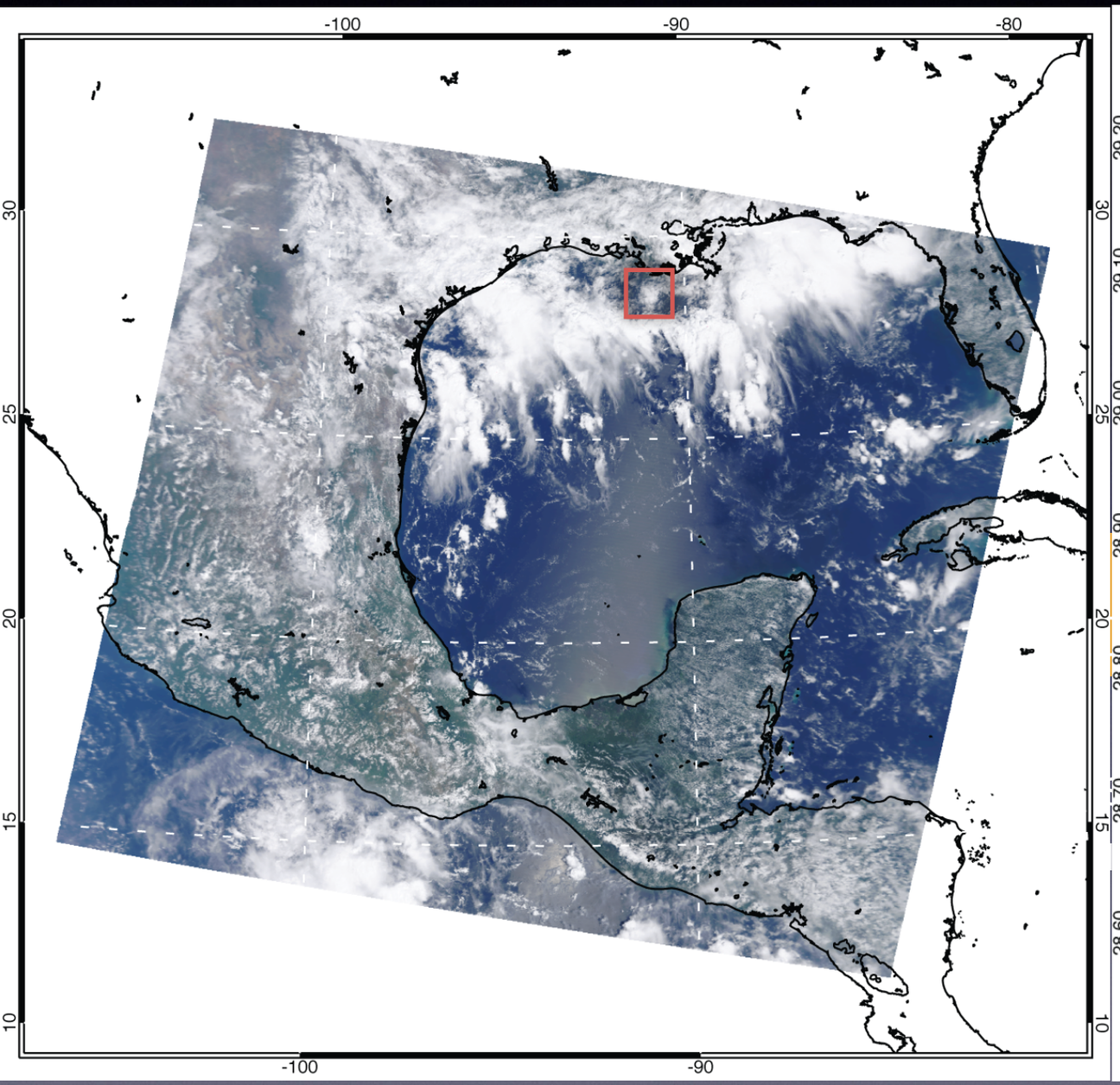

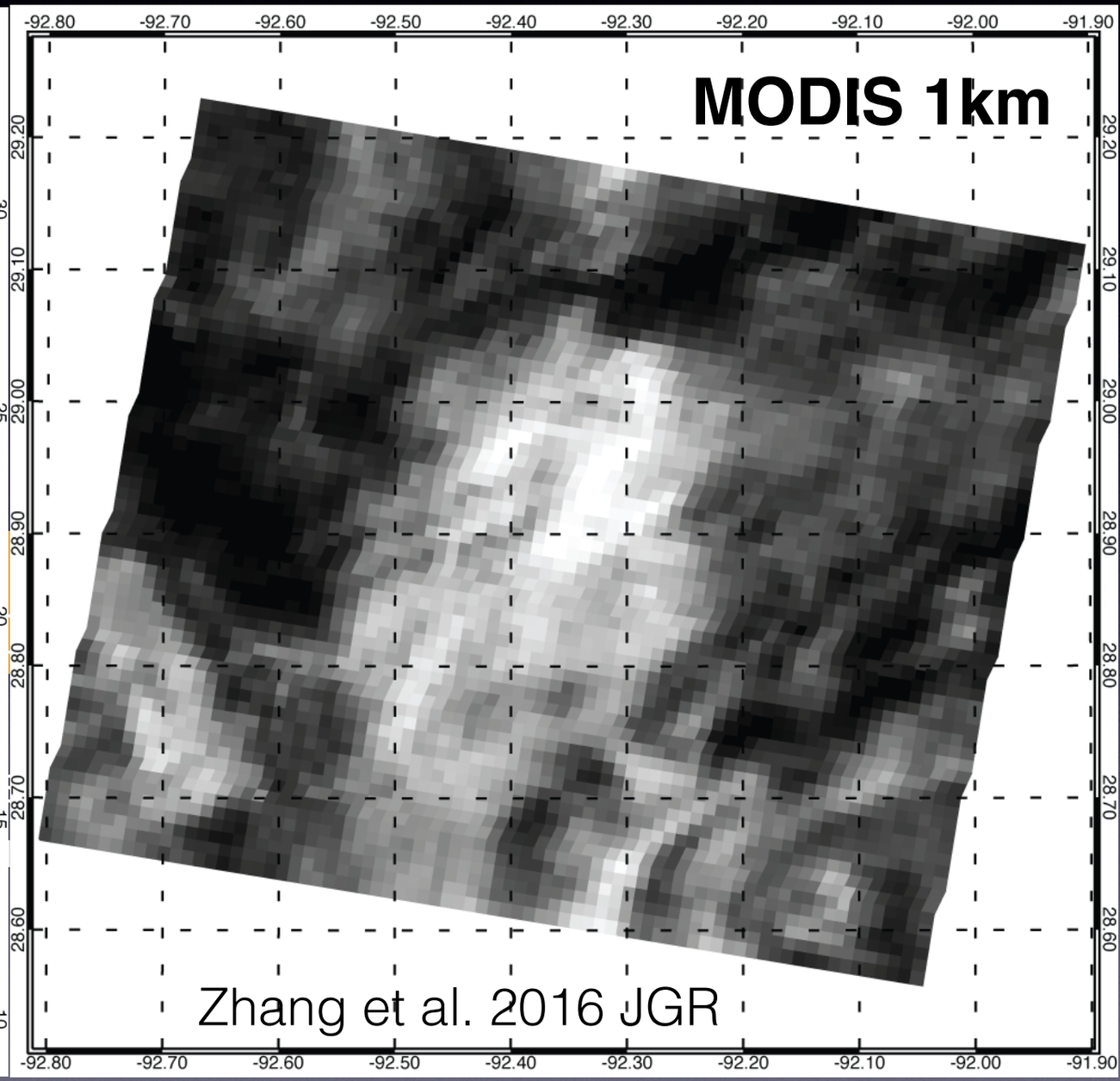

Retrieval based on averaged reflectance — average of sub pixel retrievals

PPHB $\Delta\tau = \tau\left(\overline{R_{VIS}}, \overline{R_{SWIR}}\right) - \overline{\tau\left(R_{VIS,i}, R_{SWIR,i}\right)}$

Retrieval based on averaged reflectance — average of sub pixel retrievals

$\Delta r_e = r_e\left(\overline{R_{VIS}}, \overline{R_{SWIR}}\right) - \overline{r_e\left(R_{VIS,i}, R_{SWIR,i}\right)}$

Horizontal Sub-pixel Inhomogeneity (SPI)

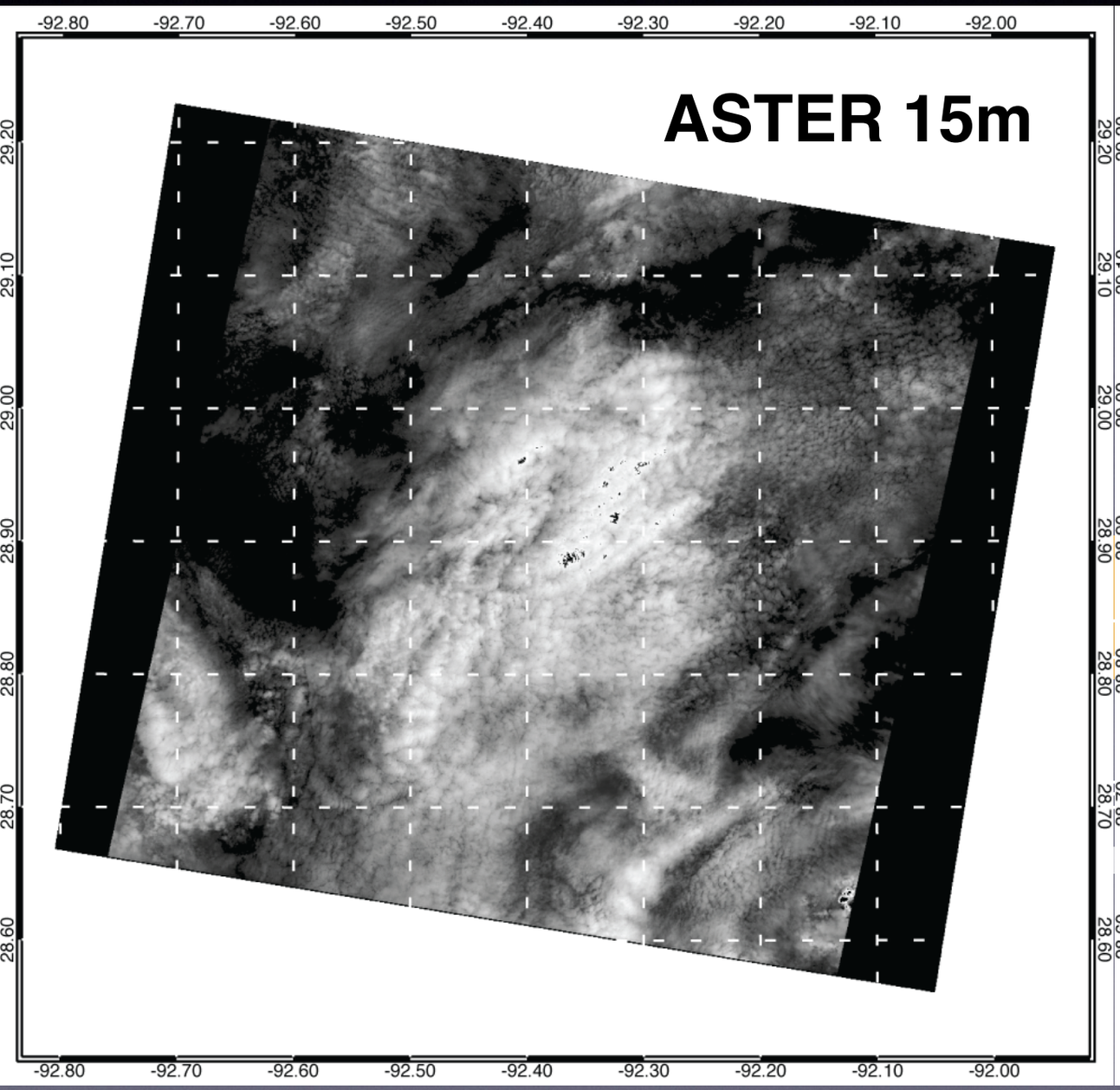

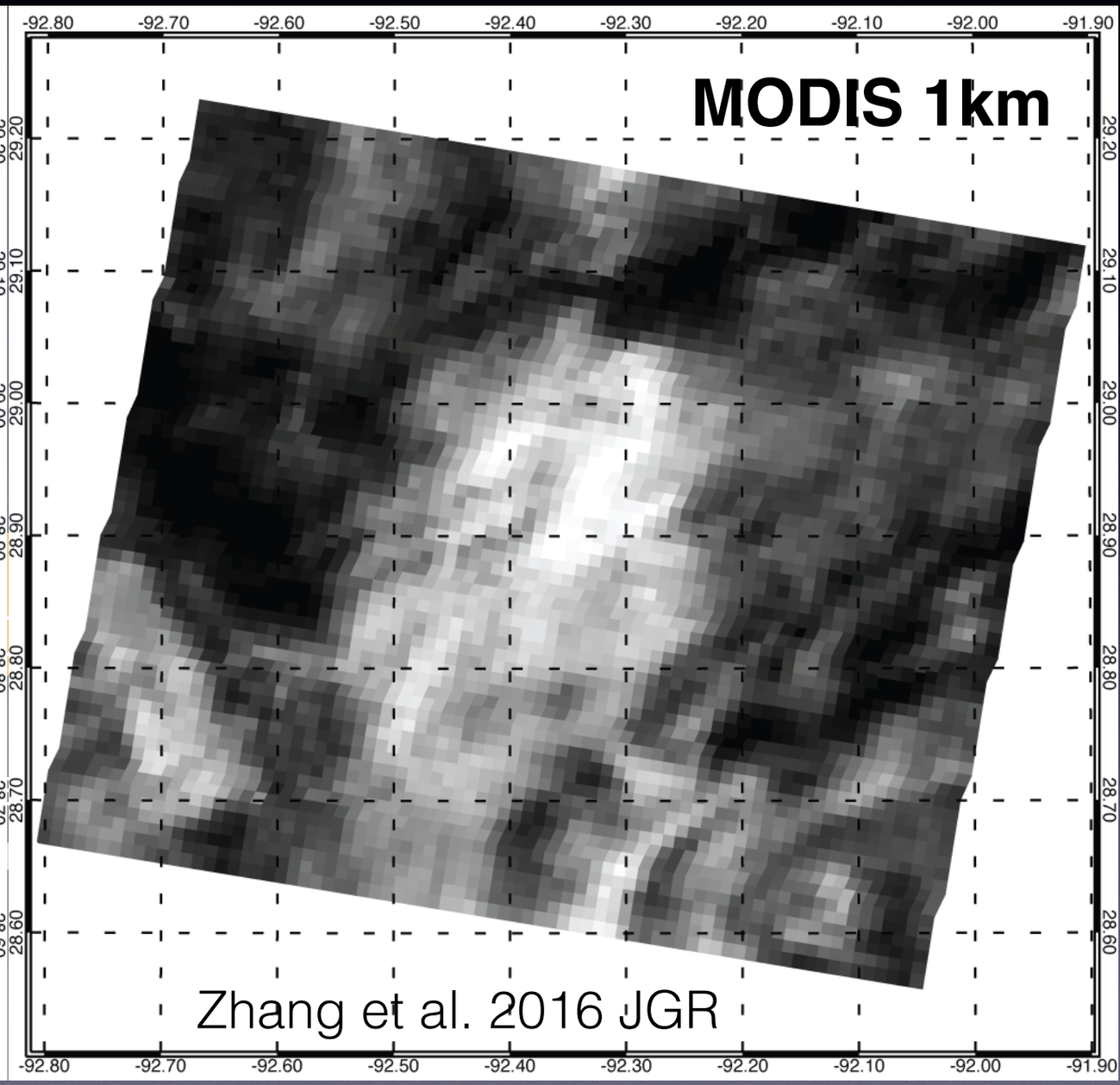

Zhang et al. 2016 JGR

PPHB $\Delta\tau = \tau\left(\overline{R_{VIS}}, \overline{R_{SWIR}}\right) - \overline{\tau\left(R_{VIS,i}, R_{SWIR,i}\right)}$

Retrieval based on averaged reflectance — average of sub pixel retrievals

$\Delta r_e = r_e\left(\overline{R_{VIS}}, \overline{R_{SWIR}}\right) - \overline{r_e\left(R_{VIS,i}, R_{SWIR,i}\right)}$

Retrieval based on averaged reflectance — average of sub pixel retrievals

Plane-parallel homogeneous bias

Marshak et al. 2006

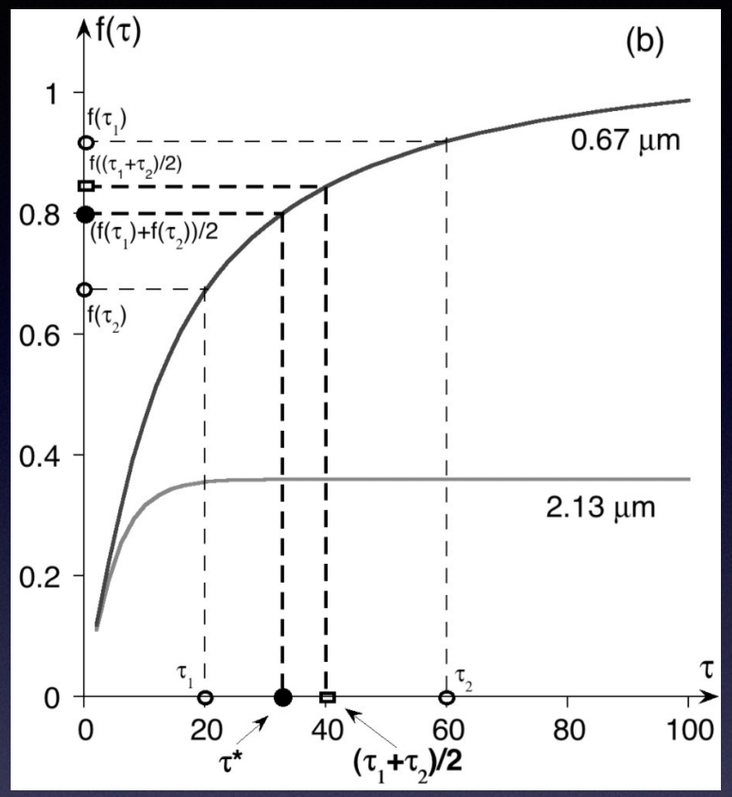

Because R_{VIS} is non-linearly dependent on COT, if a pixel is inhomogeneous the retrieved COT based on the averaged reflectance is smaller than the sub-pixel mean COT

$$\frac{\partial^2 R_{VIS}}{\partial \tau^2} \neq 0$$

$$\overline{R_{VIS}} = \left[R_{VIS}(\tau_1) + R_{VIS}(\tau_2) \right] / 2$$

$$\tau^* \left(\overline{R_{VIS}} \right) < \left(\tau_1 + \tau_2 \right) / 2$$

<u>Underlying assumption:</u>
COT and CER retrievals are mutually independent

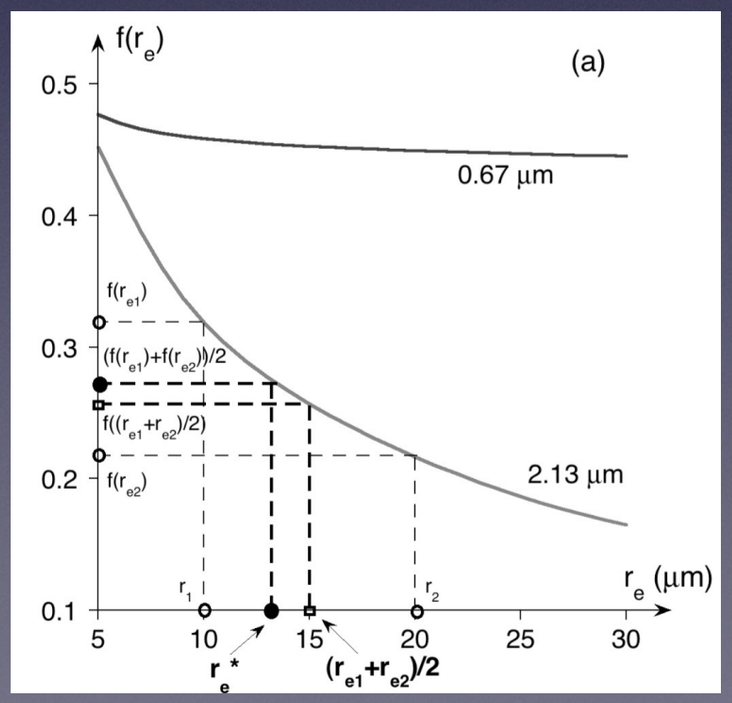

Because R_{SWIR} is non-linearly dependent on CER, if a pixel is inhomogeneous the retrieved CER based on the averaged reflectance is smaller than the sub-pixel mean CER

$$\frac{\partial^2 R_{SWIR}}{\partial r_e^2} \neq 0$$

$$\overline{R_{SWIR}} = \left[R_{SWIR}(r_{e,1}) + R_{SWIR}(r_{e,1}) \right] / 2$$

$$r_e^* \left(\overline{R_{SWIR}} \right) < \left(r_{e,1} + r_{e,1} \right) / 2$$

Plane-parallel homogeneous bias

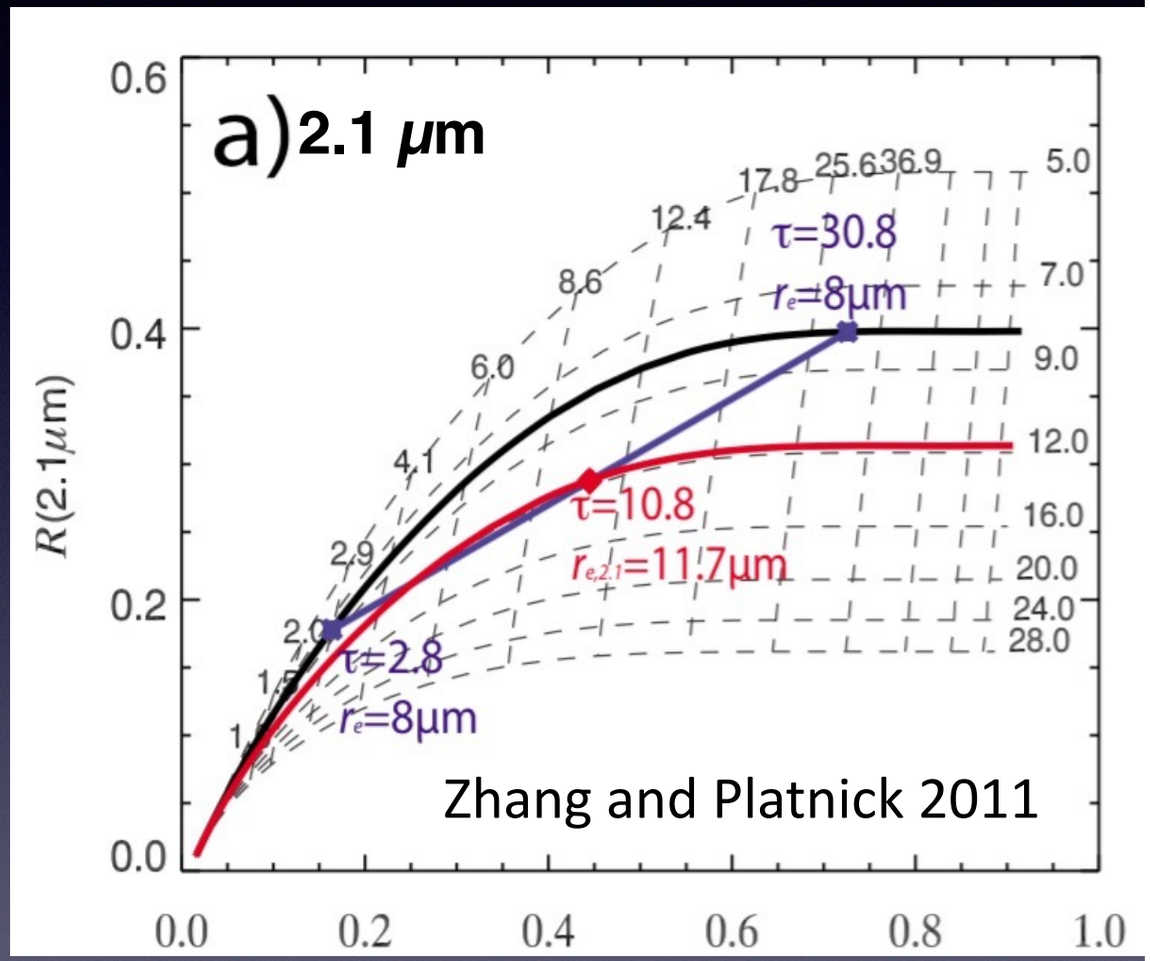

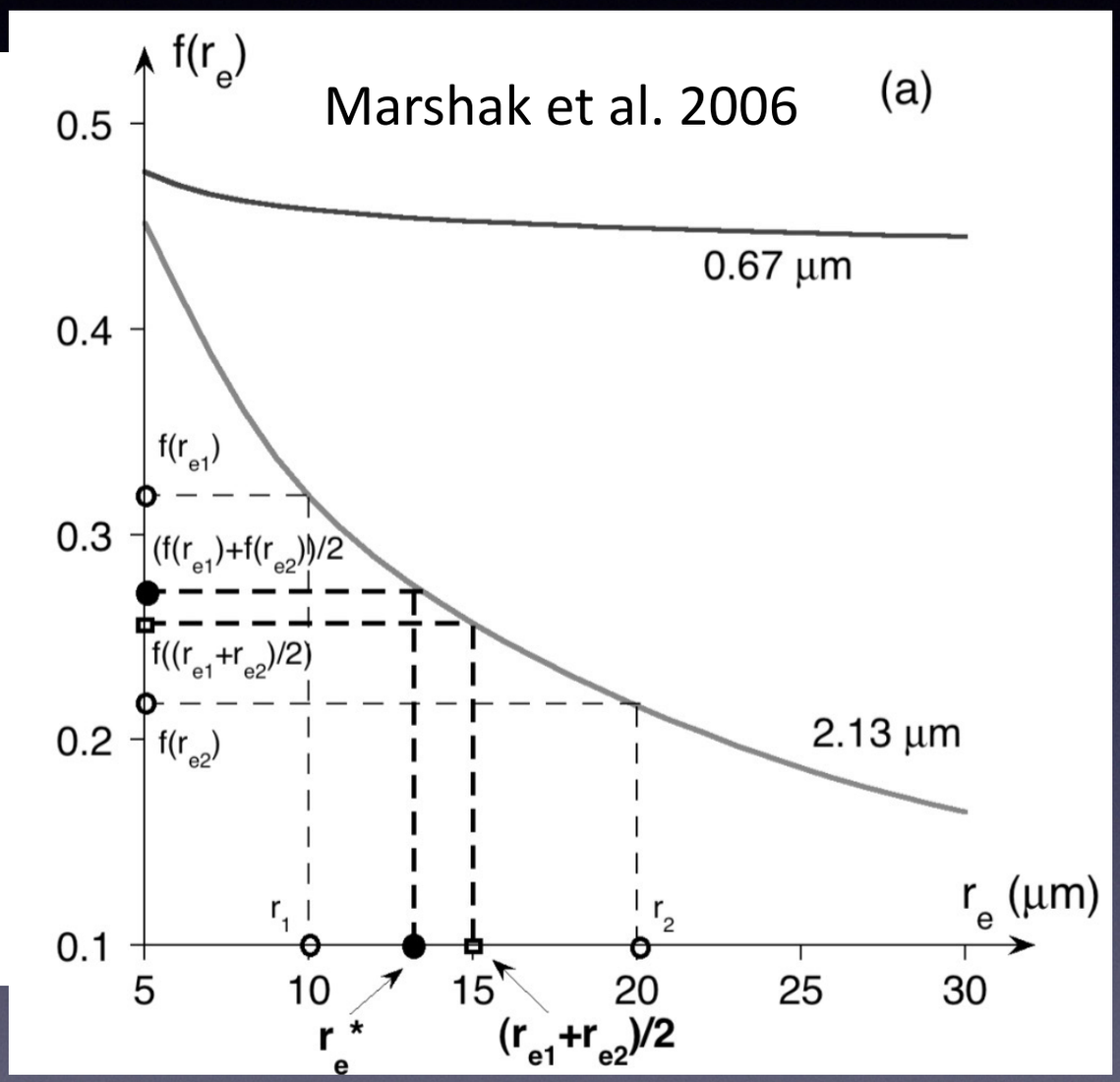

$$r_e^* > \left(r_{e,1} + r_{e,1}\right)/2$$

$$r_e^* < \left(r_{e,1} + r_{e,1}\right)/2$$

A unified framework for quantifying PPHB based on 2-D Taylor expansion

Zhang et al. 2016 JGR (in press)

$$\tau \equiv \tau\left(R_{VIS}, R_{SWIR}\right)$$
$$r_e \equiv r_e\left(R_{VIS}, R_{SWIR}\right)$$

sub-pixel pixel mean

$$R_{VIS,i} = \overline{R_{VIS}} + \Delta R_{VIS,i}$$
$$R_{SWIR,i} = \overline{R_{SWIR}} + \Delta R_{SWIR,i} \quad ; i = 1,2...N$$

$$\overline{\Delta R_{VIS,i}} = 0$$
$$\overline{\Delta R_{SWIR,i}} = 0$$

Plane-parallel homogeneous bias

$$\Delta\tau = \tau\left(\overline{R_{VIS}}, \overline{R_{SWIR}}\right) - \overline{\tau\left(R_{VIS,i}, R_{SWIR,i}\right)}$$
$$\Delta r_e = r_e\left(\overline{R_{VIS}}, \overline{R_{SWIR}}\right) - \overline{r_e\left(R_{VIS,i}, R_{SWIR,i}\right)}$$

Taylor expansion of two-variable function

$$r_e\left(R_{VIS,i}, R_{SWIR,i}\right) = r_e\left(\overline{R_{VIS}} + \Delta R_{VIS,i}, \overline{R_{SWIR}} + \Delta R_{SWIR,i}\right)$$
$$= r_e\left(\overline{R_{VIS}}, \overline{R_{SWIR}}\right) + \underbrace{\frac{\partial r_e\left(\overline{R_{VIS}}, \overline{R_{SWIR}}\right)}{\partial R_{VIS}} \Delta R_{VIS,i} + \frac{\partial r_e\left(\overline{R_{VIS}}, \overline{R_{SWIR}}\right)}{\partial R_{SWIR}} \Delta R_{SWIR,i}}_{\text{Linear terms}} +$$
$$\underbrace{\frac{1}{2}\frac{\partial^2 r_e\left(\overline{R_{VIS}}, \overline{R_{SWIR}}\right)}{\partial R_{VIS}^2} \Delta R_{VIS,i}^2 + \frac{\partial^2 r_e\left(\overline{R_{VIS}}, \overline{R_{SWIR}}\right)}{\partial R_{VIS}\,\partial R_{SWIR}} \Delta R_{VIS,i}\Delta R_{SWIR,i} + \frac{1}{2}\frac{\partial^2 r_e\left(\overline{R_{VIS}}, \overline{R_{SWIR}}\right)}{\partial R_{SWIR}^2} \Delta R_{SWIR,i}^2}_{\text{Second-order terms}} + \varepsilon$$

A unified framework for quantifying PPHB based on 2-D Taylor expansion

Zhang et al. 2016 JGR (in press)

$$\tau \equiv \tau\left(R_{VIS}, R_{SWIR}\right)$$

$$r_e \equiv r_e\left(R_{VIS}, R_{SWIR}\right)$$

sub-pixel pixel mean

$$R_{VIS,i} = \overline{R_{VIS}} + \Delta R_{VIS,i}$$

$$R_{SWIR,i} = \overline{R_{SWIR}} + \Delta R_{SWIR,i}$$

$$;i = 1,2...N$$

$$\overline{\Delta R_{VIS,i}} = 0$$

$$\overline{\Delta R_{SWIR,i}} = 0$$

Plane-parallel homogeneous bias

$$\Delta\tau = \tau\left(\overline{R_{VIS}}, \overline{R_{SWIR}}\right) - \overline{\tau\left(R_{VIS,i}, R_{SWIR,i}\right)}$$

$$\Delta r_e = r_e\left(\overline{R_{VIS}}, \overline{R_{SWIR}}\right) - \overline{r_e\left(R_{VIS,i}, R_{SWIR,i}\right)}$$

$$\overline{\tau\left(R_{VIS,i}, R_{SWIR,i}\right)} \approx \tau\left(\overline{R_{VIS}}, \overline{R_{SWIR}}\right) + \frac{1}{2}\frac{\partial^2\tau\left(\overline{R_{VIS}}, \overline{R_{SWIR}}\right)}{\partial R_{VIS}^2}\sigma_{VIS}^2 + \frac{\partial^2\tau\left(\overline{R_{VIS}}, \overline{R_{SWIR}}\right)}{\partial R_{VIS}\,\partial R_{SWIR}}\mathrm{cov}\left(R_{VIS}, R_{SWIR}\right) + \frac{1}{2}\frac{\partial^2\tau\left(\overline{R_{VIS}}, \overline{R_{SWIR}}\right)}{\partial R_{SWIR}^2}\sigma_{SWIR}^2$$

$$\overline{r_e\left(R_{VIS,i}, R_{SWIR,i}\right)} \approx r_e\left(\overline{R_{VIS}}, \overline{R_{SWIR}}\right) + \frac{1}{2}\frac{\partial^2 r_e\left(\overline{R_{VIS}}, \overline{R_{SWIR}}\right)}{\partial R_{VIS}^2}\sigma_{VIS}^2 + \frac{\partial^2 r_e\left(\overline{R_{VIS}}, \overline{R_{SWIR}}\right)}{\partial R_{VIS}\,\partial R_{SWIR}}\mathrm{cov}\left(R_{VIS}, R_{SWIR}\right) + \frac{1}{2}\frac{\partial^2 r_e\left(\overline{R_{VIS}}, \overline{R_{SWIR}}\right)}{\partial R_{SWIR}^2}\sigma_{SWIR}^2$$

A unified framework for quantifying PPHB based on 2-D Taylor expansion

Zhang et al. 2016 JGR (in press)

$$\tau \equiv \tau\left(R_{VIS}, R_{SWIR}\right)$$

$$r_e \equiv r_e\left(R_{VIS}, R_{SWIR}\right)$$

sub-pixel pixel mean

$$R_{VIS,i} = \overline{R_{VIS}} + \Delta R_{VIS,i}$$

$$R_{SWIR,i} = \overline{R_{SWIR}} + \Delta R_{SWIR,i}$$

$$;i = 1,2...N$$

$$\overline{\Delta R_{VIS,i}} = 0$$

$$\overline{\Delta R_{SWIR,i}} = 0$$

Plane-parallel homogeneous bias

$$\Delta\tau = \tau\left(\overline{R_{VIS}}, \overline{R_{SWIR}}\right) - \overline{\tau\left(R_{VIS,i}, R_{SWIR,i}\right)}$$

$$\Delta r_e = r_e\left(\overline{R_{VIS}}, \overline{R_{SWIR}}\right) - \overline{r_e\left(R_{VIS,i}, R_{SWIR,i}\right)}$$

PPHB Inhomogeneity matrix SPI

$$\begin{pmatrix} \Delta\tau \\ \Delta r_e \end{pmatrix} = \begin{pmatrix} -\frac{1}{2}\frac{\partial^2\tau\left(\overline{R_{VIS}}, \overline{R_{SWIR}}\right)}{\partial R_{VIS}^2} & -\frac{\partial^2\tau\left(\overline{R_{VIS}}, \overline{R_{SWIR}}\right)}{\partial R_{VIS}\,\partial R_{SWIR}} & -\frac{1}{2}\frac{\partial^2\tau\left(\overline{R_{VIS}}, \overline{R_{SWIR}}\right)}{\partial R_{SWIR}^2} \\ -\frac{1}{2}\frac{\partial^2 r_e\left(\overline{R_{VIS}}, \overline{R_{SWIR}}\right)}{\partial R_{VIS}^2} & -\frac{\partial^2 r_e\left(\overline{R_{VIS}}, \overline{R_{SWIR}}\right)}{\partial R_{VIS}\,\partial R_{SWIR}} & -\frac{1}{2}\frac{\partial^2 r_e\left(\overline{R_{VIS}}, \overline{R_{SWIR}}\right)}{\partial R_{SWIR}^2} \end{pmatrix} \begin{pmatrix} \sigma_{VIS}^2 \\ \mathrm{cov} \\ \sigma_{SWIR}^2 \end{pmatrix}$$

inherent sensitivity actual SPI

A unified framework for quantifying PPHB based on 2-D Taylor expansion

Zhang et al. 2016 JGR (in press)

$$\begin{pmatrix} \Delta\tau \\ \Delta r_e \end{pmatrix} = \begin{pmatrix} -\frac{1}{2}\frac{\partial^2\tau\left(\overline{R_{VIS}},\overline{R_{SWIR}}\right)}{\partial R_{VIS}^2} & -\frac{\partial^2\tau\left(\overline{R_{VIS}},\overline{R_{SWIR}}\right)}{\partial R_{VIS}\,\partial R_{SWIR}} & -\frac{1}{2}\frac{\partial^2\tau\left(\overline{R_{VIS}},\overline{R_{SWIR}}\right)}{\partial R_{SWIR}^2} \\ -\frac{1}{2}\frac{\partial^2 r_e\left(\overline{R_{VIS}},\overline{R_{SWIR}}\right)}{\partial R_{VIS}^2} & -\frac{\partial^2 r_e\left(\overline{R_{VIS}},\overline{R_{SWIR}}\right)}{\partial R_{VIS}\,\partial R_{SWIR}} & -\frac{1}{2}\frac{\partial^2 r_e\left(\overline{R_{VIS}},\overline{R_{SWIR}}\right)}{\partial R_{SWIR}^2} \end{pmatrix} \begin{pmatrix} \sigma_{VIS}^2 \\ \mathrm{cov} \\ \sigma_{SWIR}^2 \end{pmatrix}$$

Marshak et al. 2006

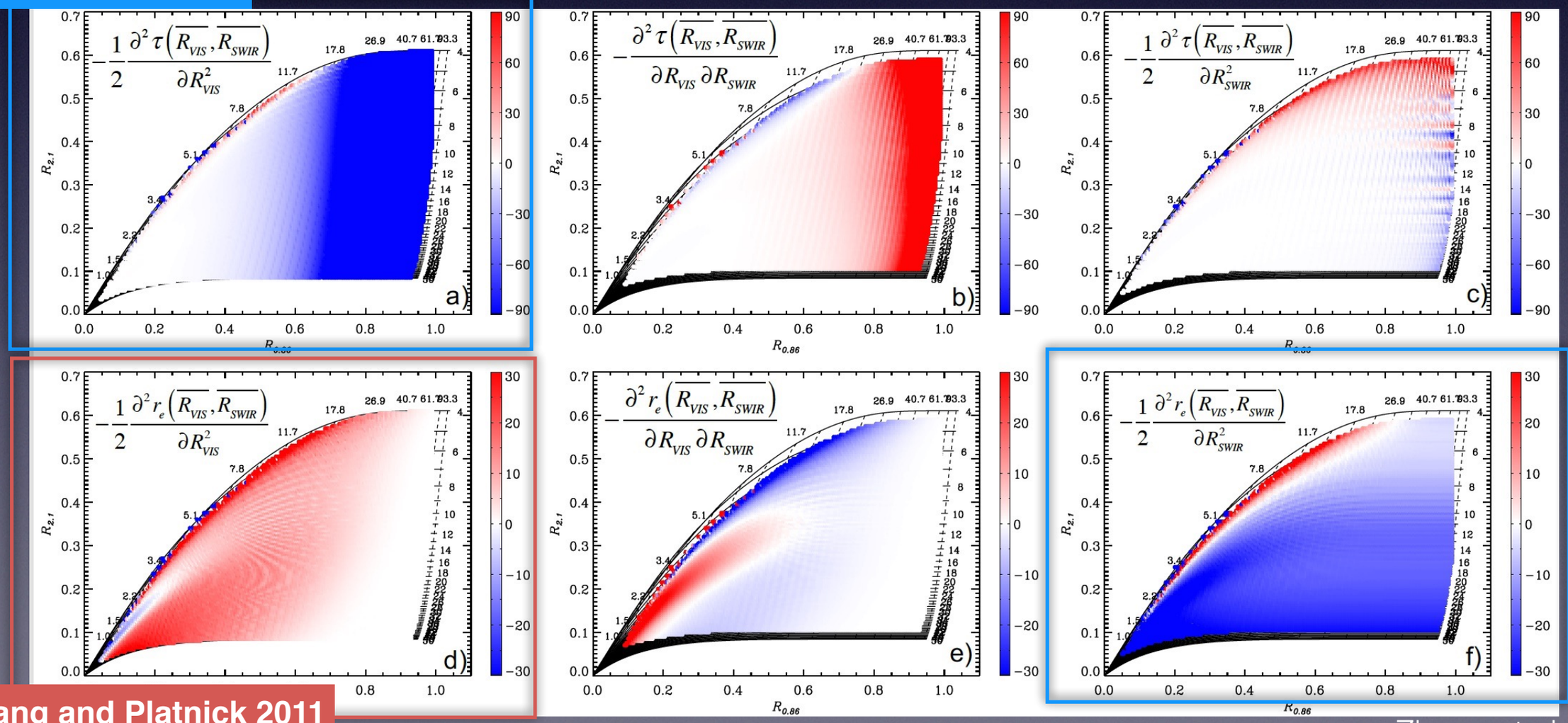

Zhang and Platnick 2011

Zhang et al. 2016

A unified framework for quantifying PPHB based on 2-D Taylor expansion

Zhang et al. 2016 JGR (in press)

$$\begin{pmatrix} \Delta\tau \\ \Delta r_e \end{pmatrix} = \begin{pmatrix} -\frac{1}{2}\frac{\partial^2\tau\left(\overline{R_{VIS}},\overline{R_{SWIR}}\right)}{\partial R_{VIS}^2} & -\frac{\partial^2\tau\left(\overline{R_{VIS}},\overline{R_{SWIR}}\right)}{\partial R_{VIS}\,\partial R_{SWIR}} & -\frac{1}{2}\frac{\partial^2\tau\left(\overline{R_{VIS}},\overline{R_{SWIR}}\right)}{\partial R_{SWIR}^2} \\ -\frac{1}{2}\frac{\partial^2 r_e\left(\overline{R_{VIS}},\overline{R_{SWIR}}\right)}{\partial R_{VIS}^2} & -\frac{\partial^2 r_e\left(\overline{R_{VIS}},\overline{R_{SWIR}}\right)}{\partial R_{VIS}\,\partial R_{SWIR}} & -\frac{1}{2}\frac{\partial^2 r_e\left(\overline{R_{VIS}},\overline{R_{SWIR}}\right)}{\partial R_{SWIR}^2} \end{pmatrix} \begin{pmatrix} \sigma_{VIS}^2 \\ \mathrm{cov} \\ \sigma_{SWIR}^2 \end{pmatrix}$$

Marshak et al. 2006

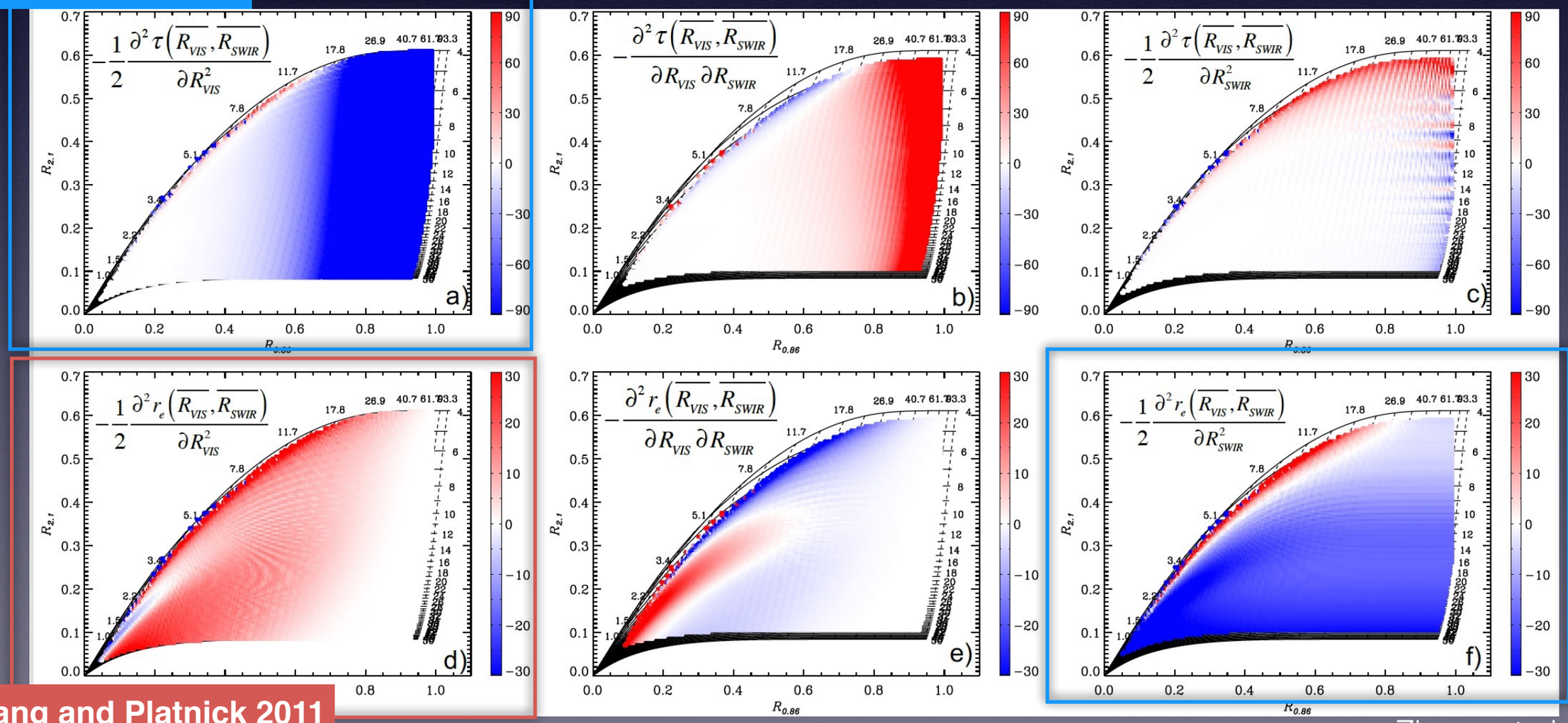

Zhang and Platnick 2011

Zhang et al. 2016

A unified framework for quantifying PPHB based on 2-D Taylor expansion

Zhang et al. 2016 JGR (in press)

$\Delta\tau$ $\Delta r_{e,2.1}$ $\Delta r_{e,3.7}$

Numerical simulation

Prediction from our framework

Correlation

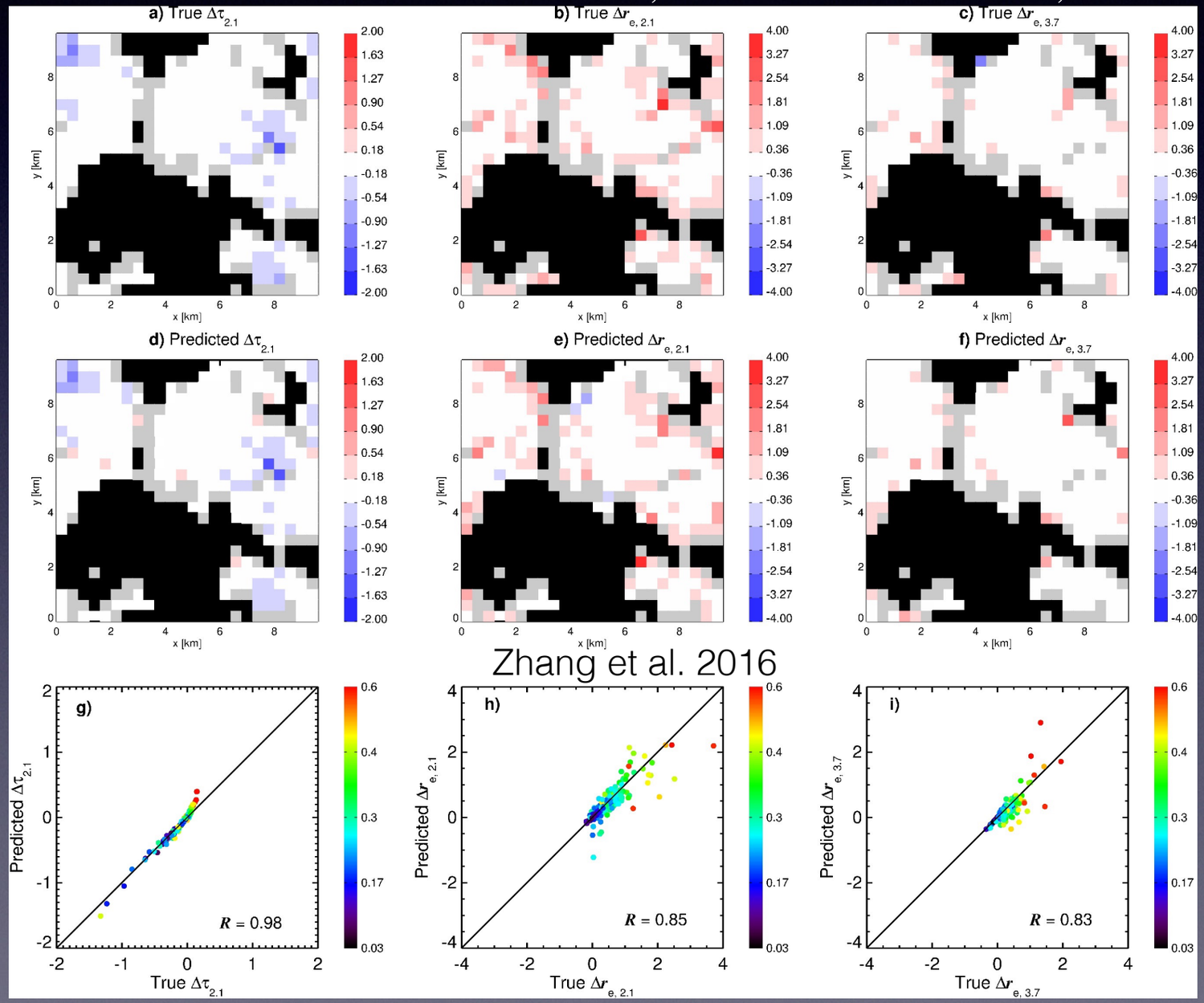

With this framework, we will be able to quantify the pixel-level uncertainty due to PPHB in the operational MODIS products!

Our new framework for the PPHB works very well in the LES case study. It is being tested using ASTER observations and global MODIS observations.

Theoretical advances II:

Impact of cloud vertical structure on MODIS LWP retrieval

$$LWP = C\rho_w \tau r_e$$

$$r_e(\tau) = r_e^* \left(\frac{\tau_{tot} - \tau}{\tau_{tot}} \right)^{\beta}$$

$$LWP = \frac{2}{3}\rho_l \int_0^{\tau_{tot}} r_e(\tau) d\tau = \frac{2}{3}\rho_l \frac{1}{\beta+1} r_e^* \tau_{tot}$$

Homogeneous cloud: β=0; C=2/3
Adiabatic cloud: β=1/5; C=5/9

Which one is better?
it depends…

Miller et al. 2016 JGR

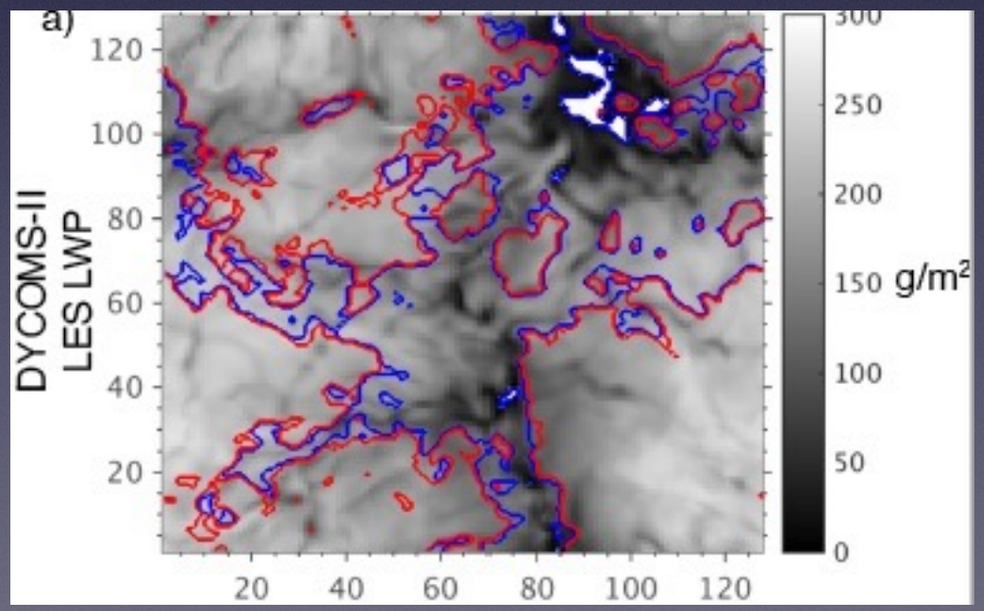

(See Dan Miller's poster)

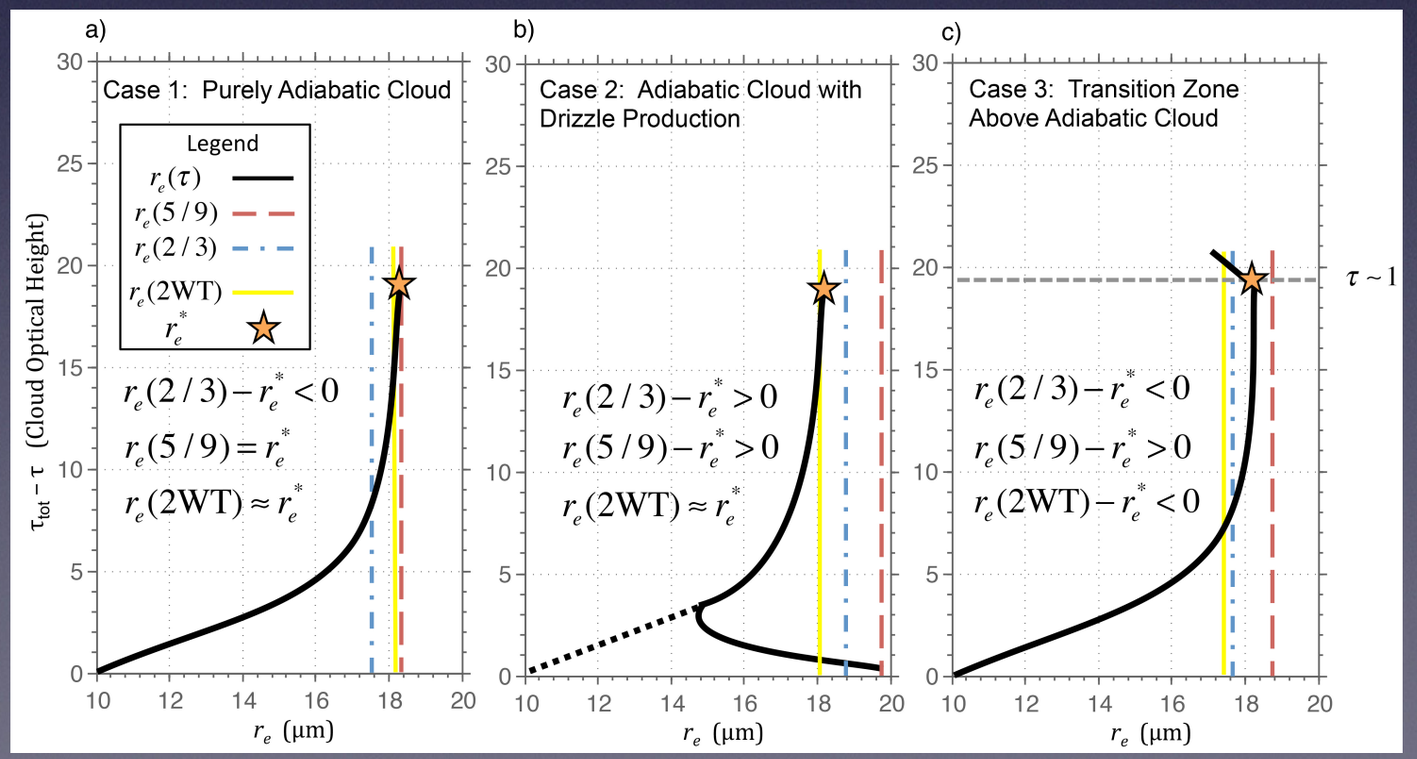

Outline

- Theory:
  - A novel framework based on 2-D Tayler expansion for quantifying the uncertainty in MODIS retrievals caused by sub-pixel reflectance inhomogeneity. (*Zhang et al. 2016)*
  - How cloud vertical structure influences MODIS LWP retrievals. (*Miller et al. 2016)*
- Observations:
  - Analysis of *failed* MODIS cloud property retrievals. *(Cho et al. 2015)*
  - Cloud property retrievals from 15m resolution ASTER observations. *(Werner et al. 2016)*
- Modeling:
  - LES-Satellite observation simulator *(Zhang et al. 2012, Miller et al. 2016)*.

Failed MODIS retrievals for MBL clouds

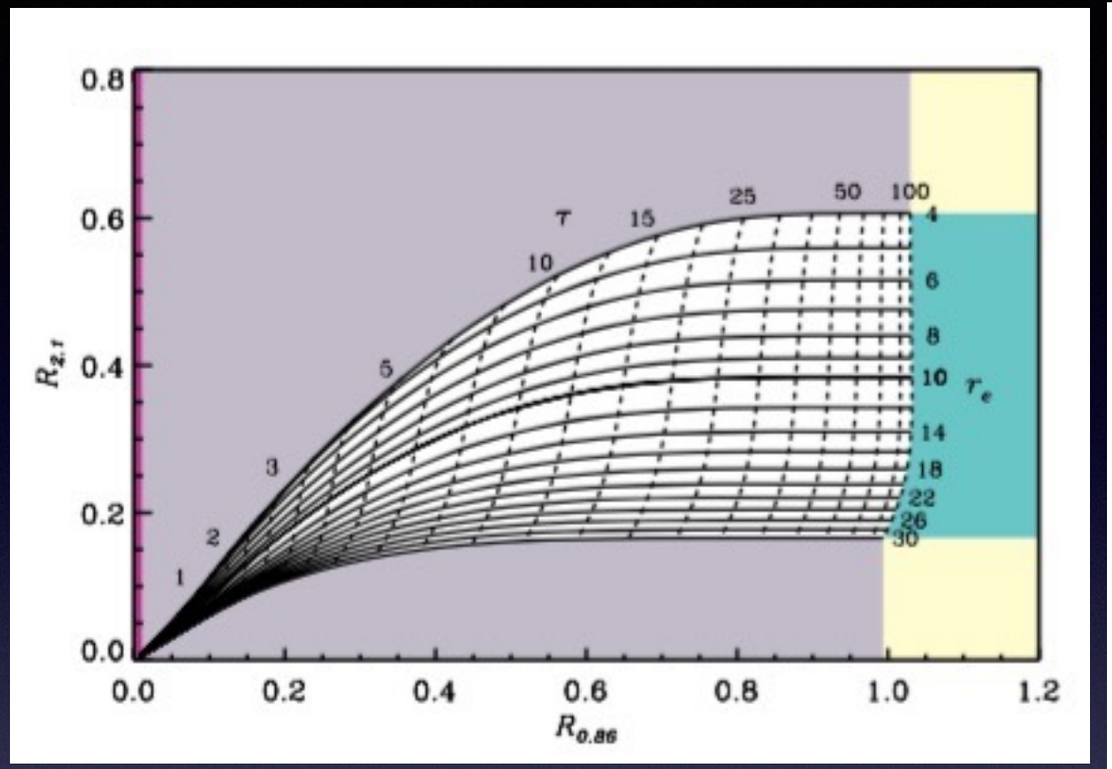

The retrieval based on the 0.86 μm and 2.1 μm MODIS channel combination has an overall failure rate of about **16%** (**10%** for the 0.86 μm and 3.7 μm combination). Failure rates can be much higher in certain regions, e.g., broken Cu.

Annual mean retrieval failure rates

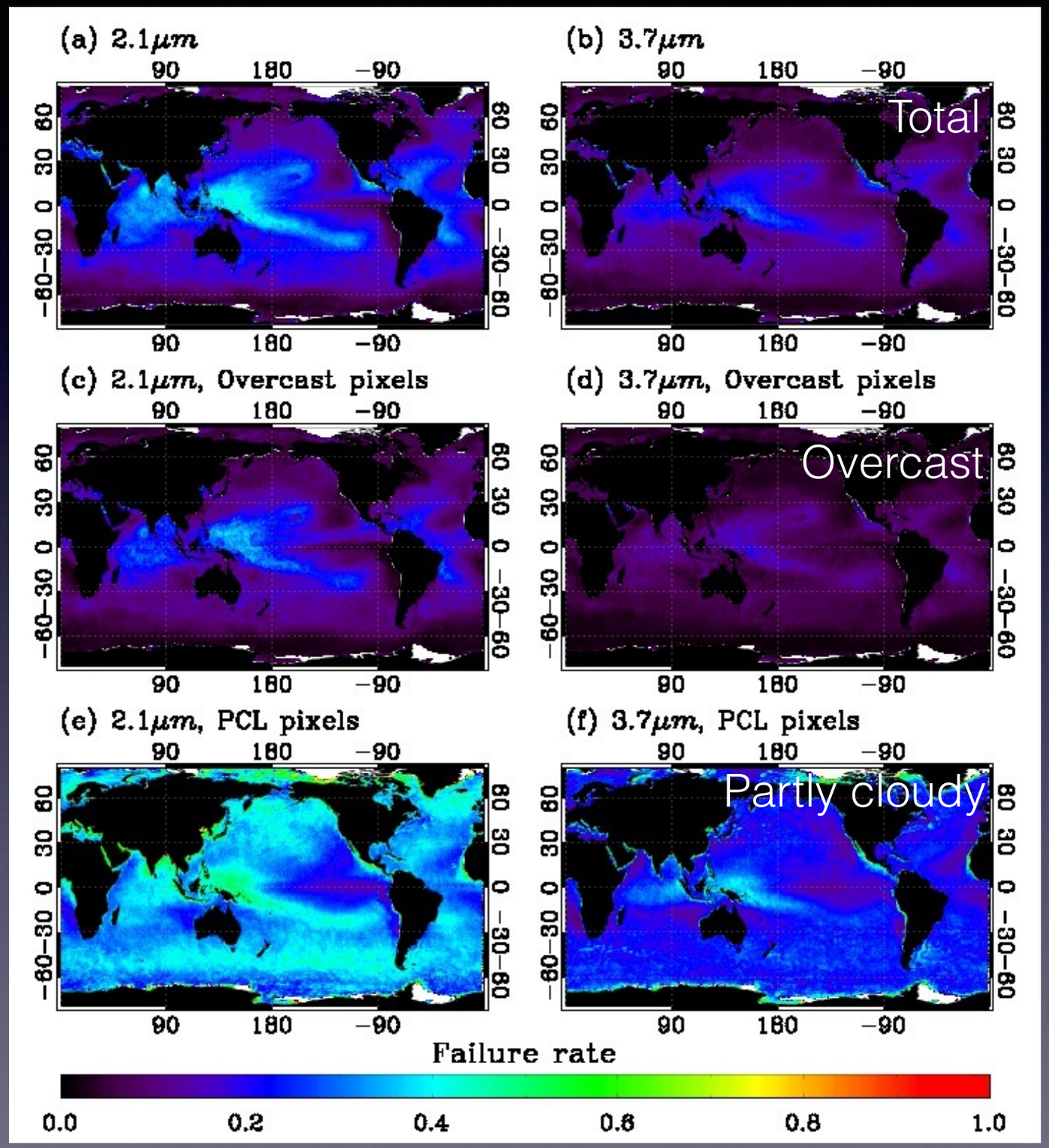

Cho et al. 2015 JGR

Cloud property retrievals from high-resolution ASTER observations

Cloud Reflectance

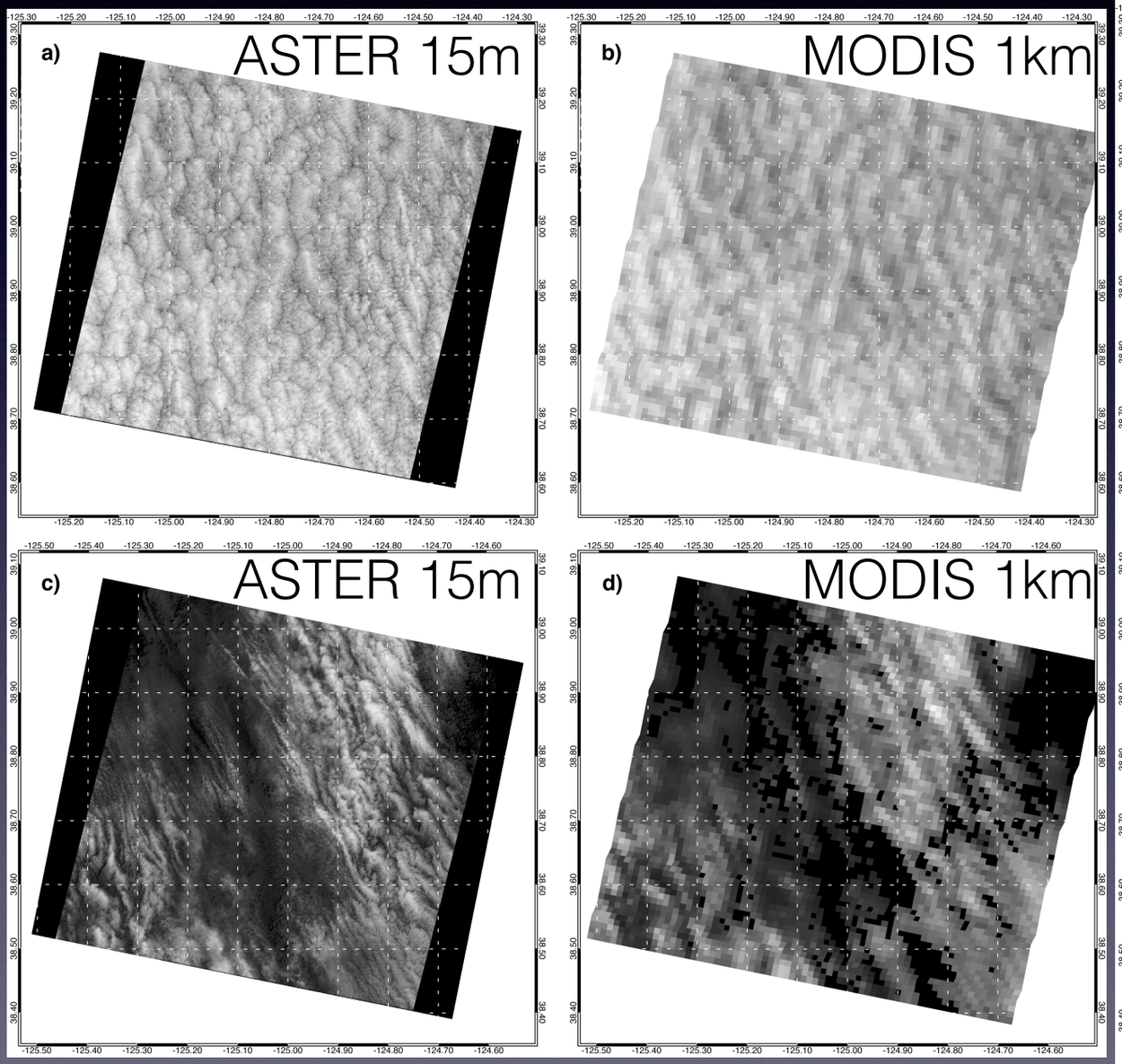

Cloud optical thickness

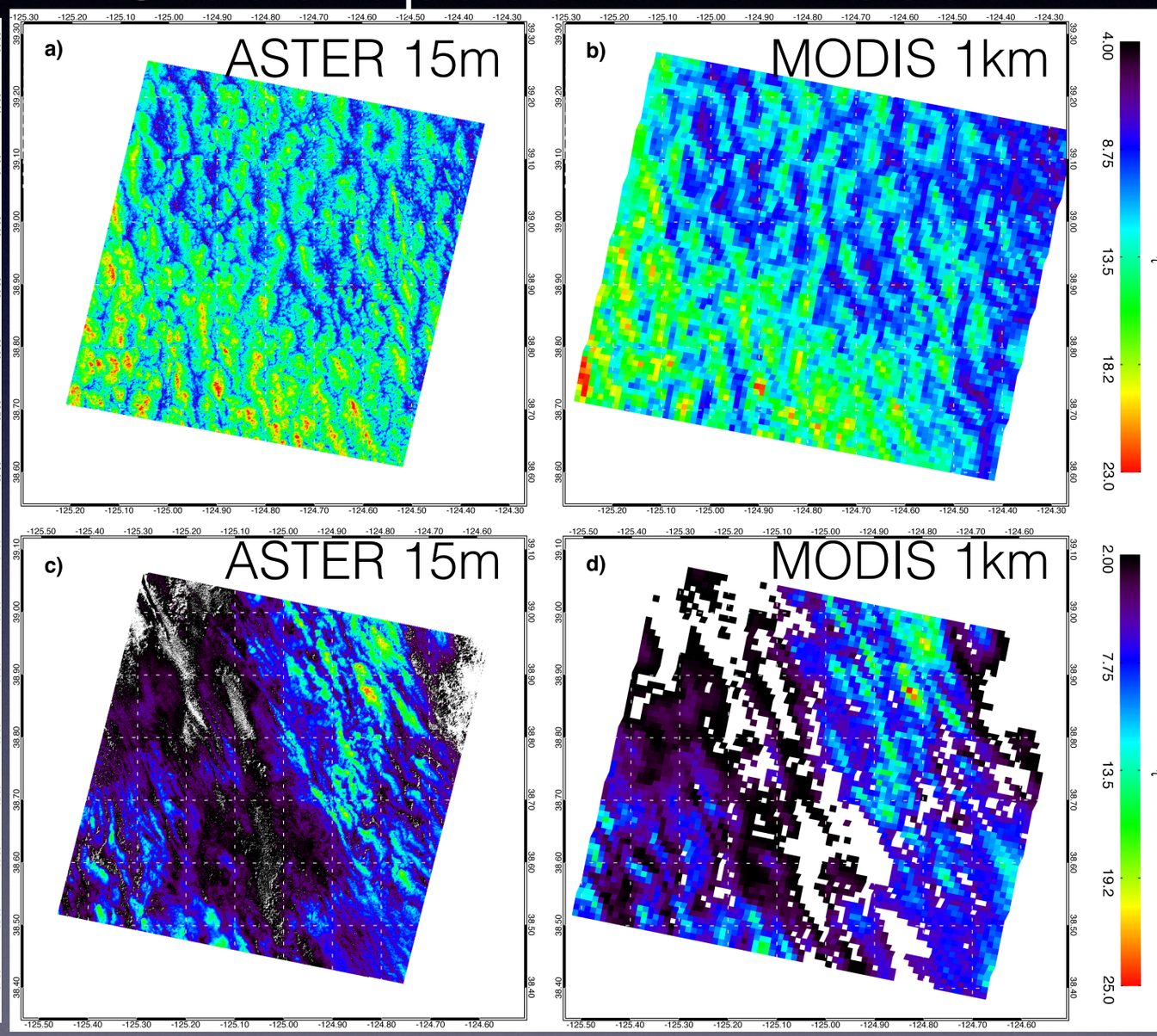

Cloud property retrievals from high-resolution ASTER observations

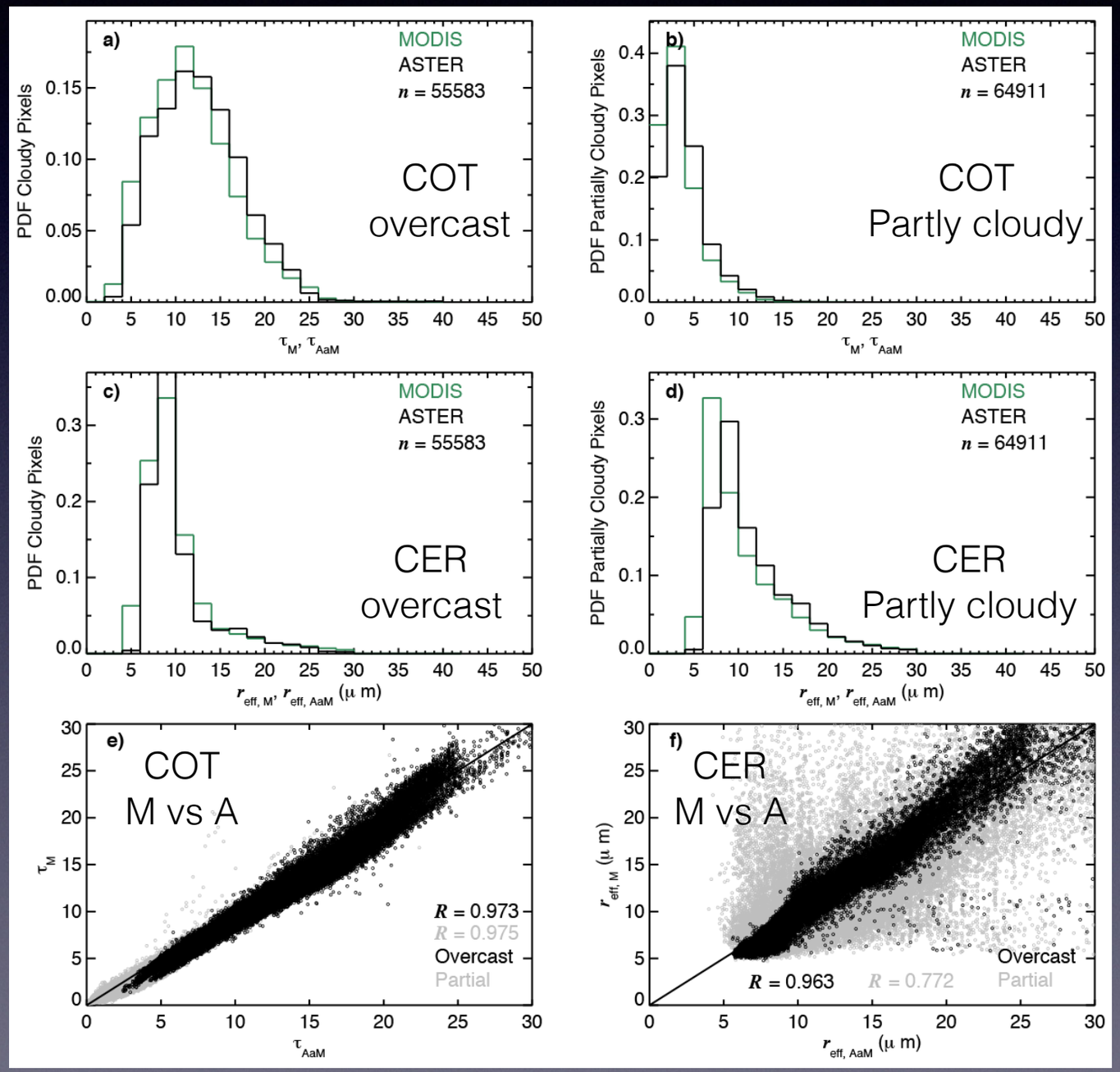

See Frank Werner's poster

Summary

- Theory:
  - A novel framework based on 2-D Tayler expansion for quantifying the uncertainty in MODIS retrievals caused by sub-pixel reflectance inhomogeneity. (*Zhang et al. 2016)*
  - How cloud vertical structure influences MODIS LWP retrievals. (*Miller et al. 2016)*
- Observation:
  - Analysis of *failed* MODIS cloud property retrievals. *(Cho et al. 2015)*
  - Cloud property retrievals from 15m resolution ASTER observations. *(Werner et al. 2016)*
- Modeling:
  - LES-Satellite observation simulator *(Zhang et al. 2012, Miller et al. 2016)*.

Thanks for your attention

- Questions?

Why are these issues important?

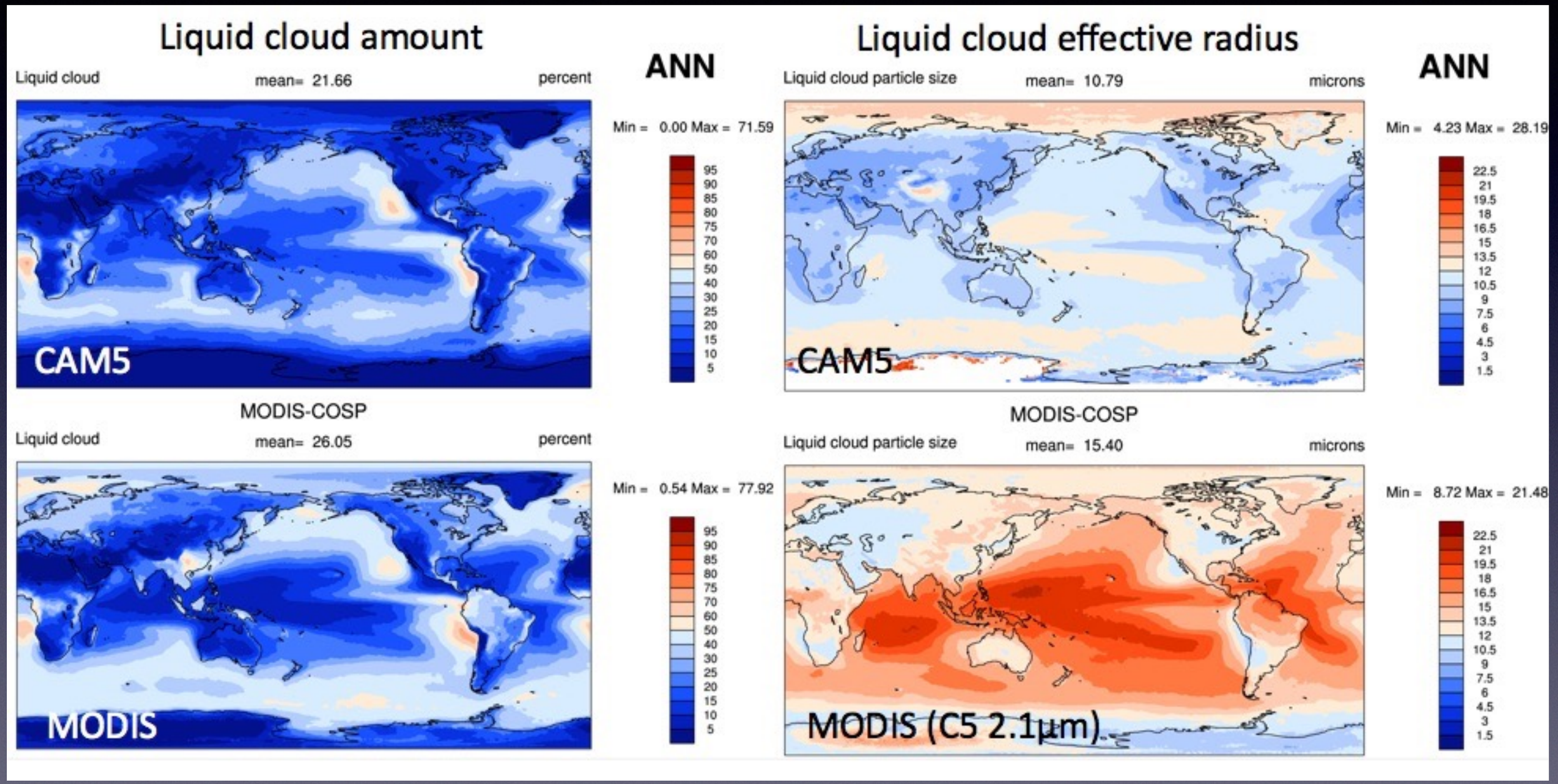

A better understanding of these issues will help us to better understand the uncertainties and potential errors in MODIS product, which hopefully could eventually lead to better simulation of MBL cloud in GCM.

Cloud Vertical Structure?

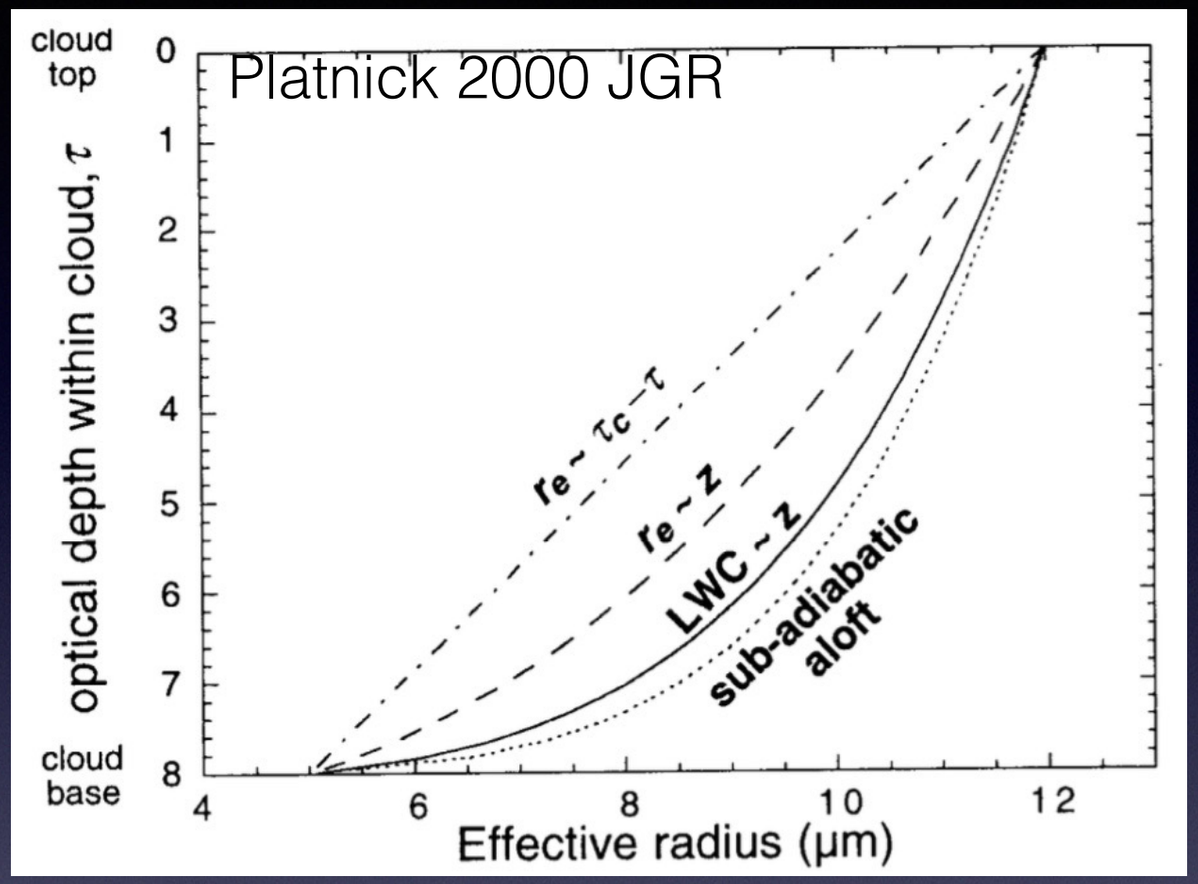

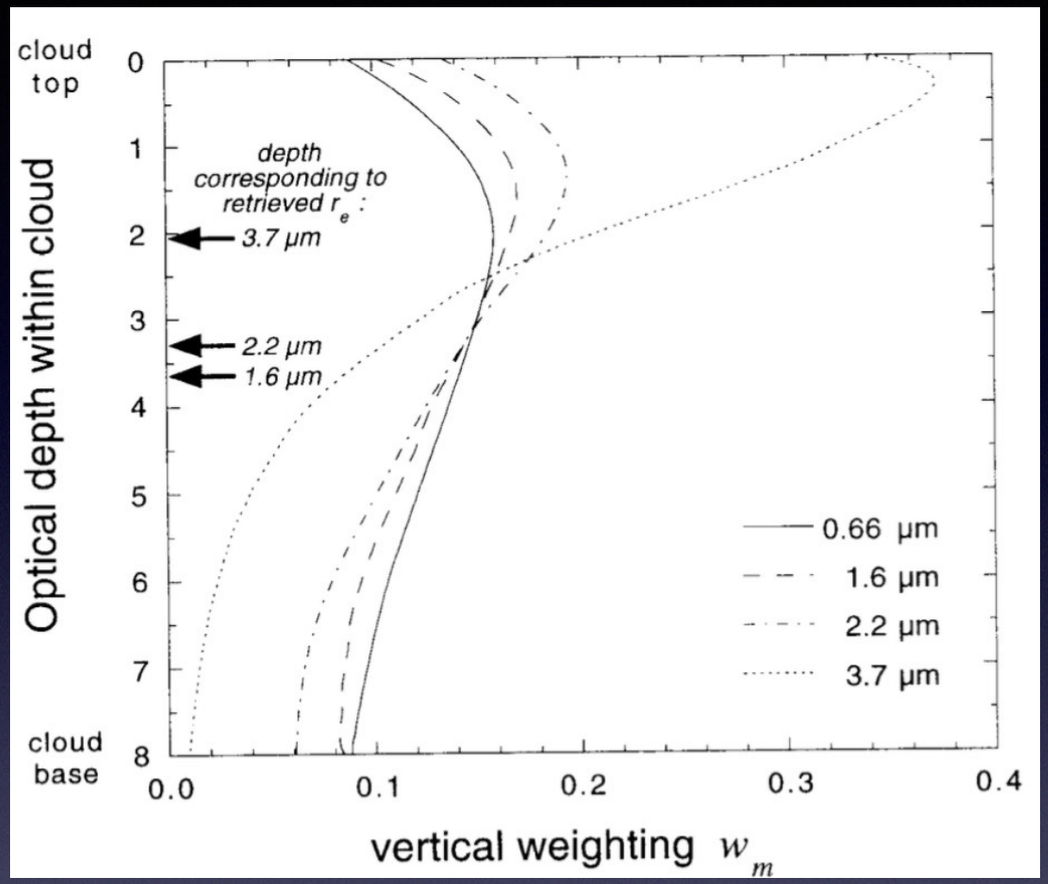

- SWIR band Cloud reflectance is more sensitive to the microphysics of cloud top than lower portion of cloud, which can be explained by the vertical weighting function.
- As predicted by the vertical weighting function, the 2.1 μm band penetrates and therefore "sees" deeper into the cloud than the 3.7 μm band.
- An important implication for retrieval is that CER2.1 < CER3.7 for pure adiabatic cloud structure.

Cloud Vertical Structure?

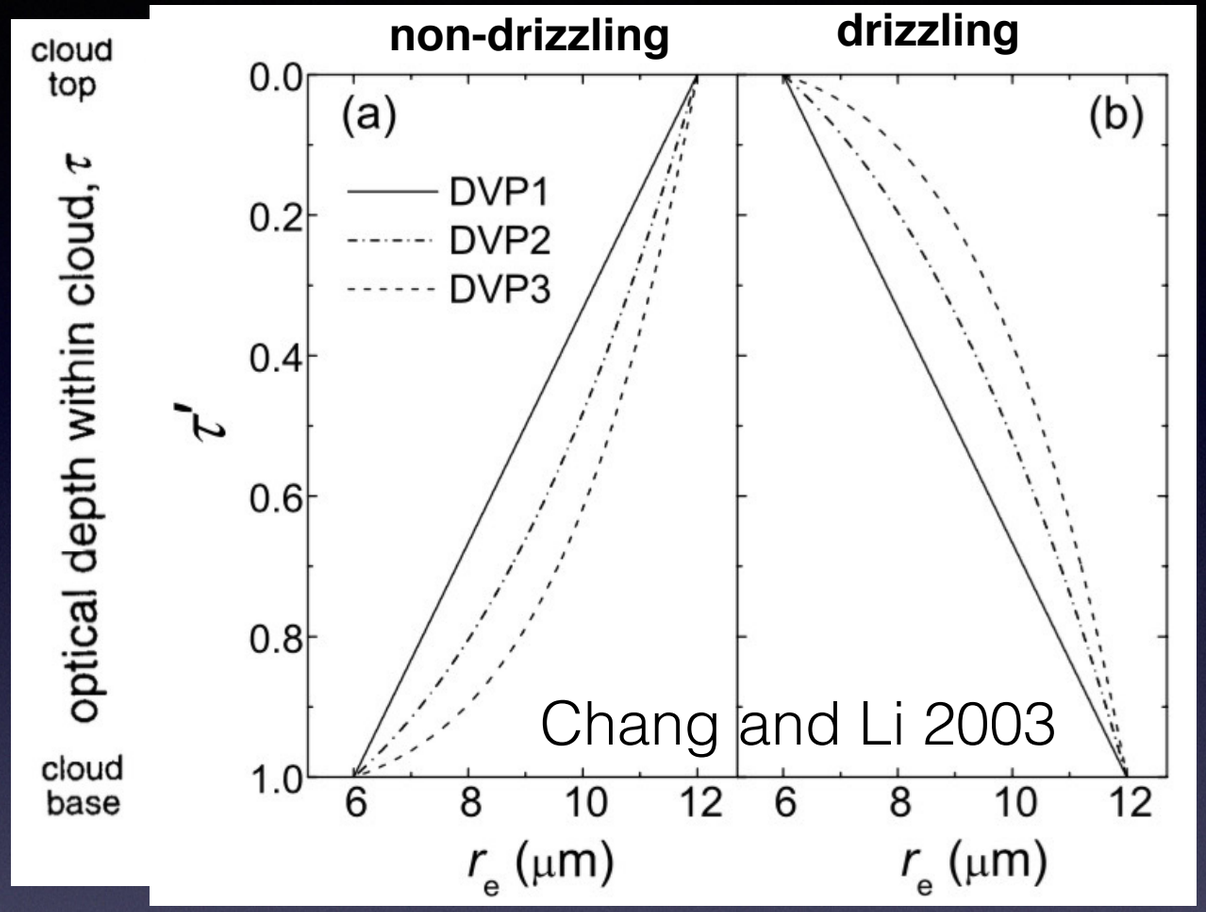

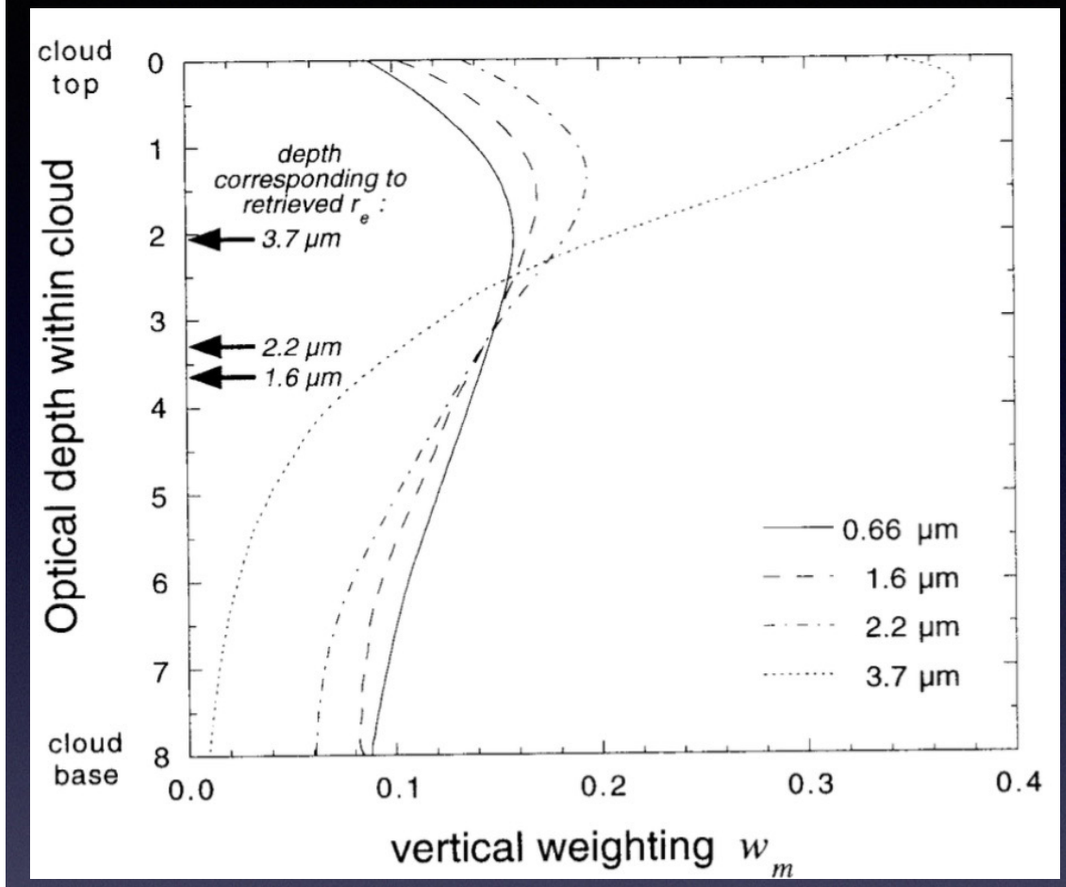

- SWIR band Cloud reflectance is more sensitive to the microphysics of cloud top than lower portion of cloud, which can be explained by the vertical weighting function.
- As predicted by the vertical weighting function, the 2.1 μm band penetrates and therefore "sees" deeper into the cloud than the 3.7 μm band.
- An important implication for retrieval is that CER2.1 < CER3.7 for pure adiabatic cloud structure.

Warm rain process leads to an increase of CER from cloud top to cloud base. 3.7 μm band has smaller penetration depth CER2.1 > CER3.7. But a large fraction of pixels with CER2.1 > CER3.7 are thin and unlikely to be drizzling

Plane-parallel homogeneous bias (PPHB)?

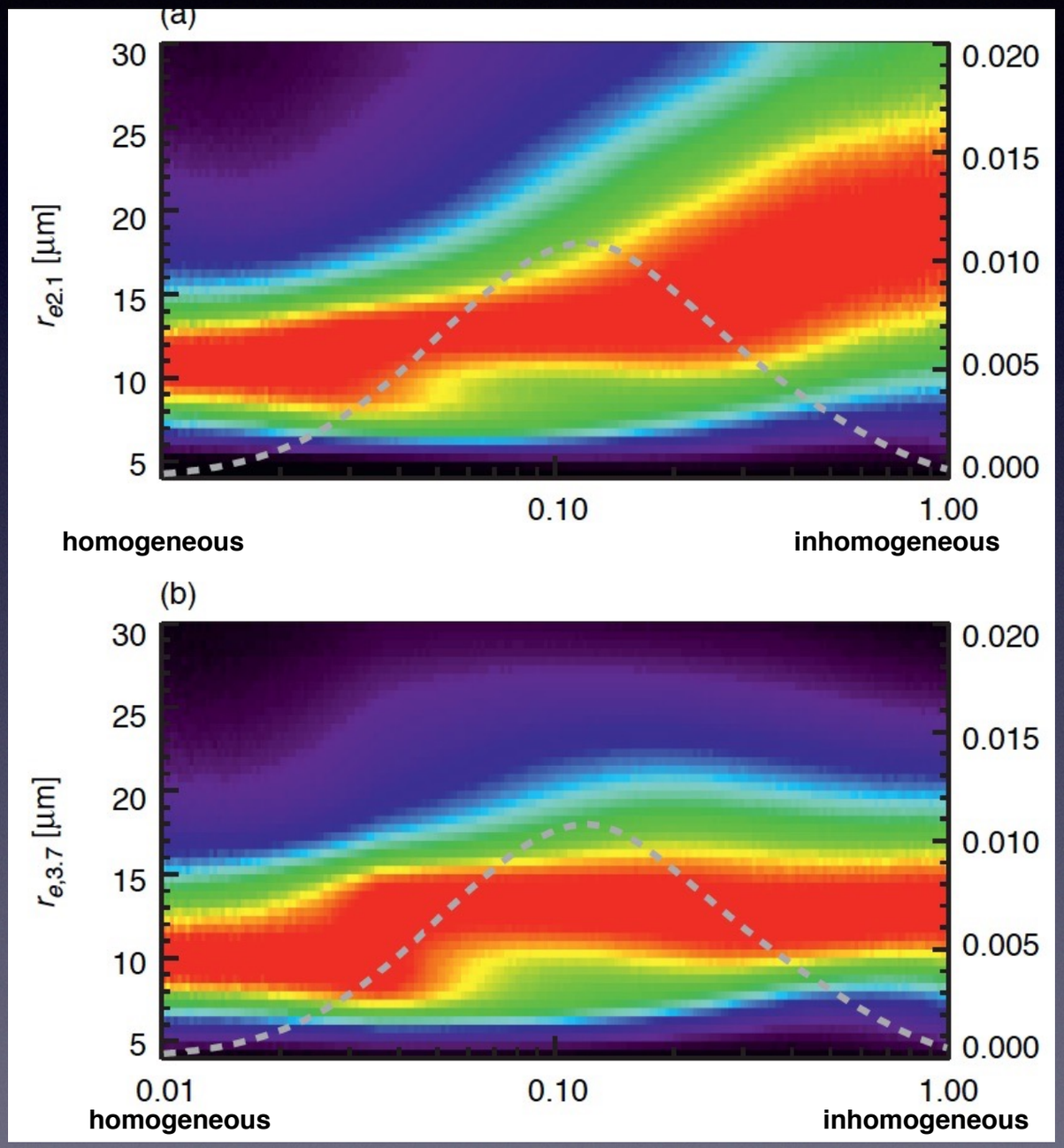

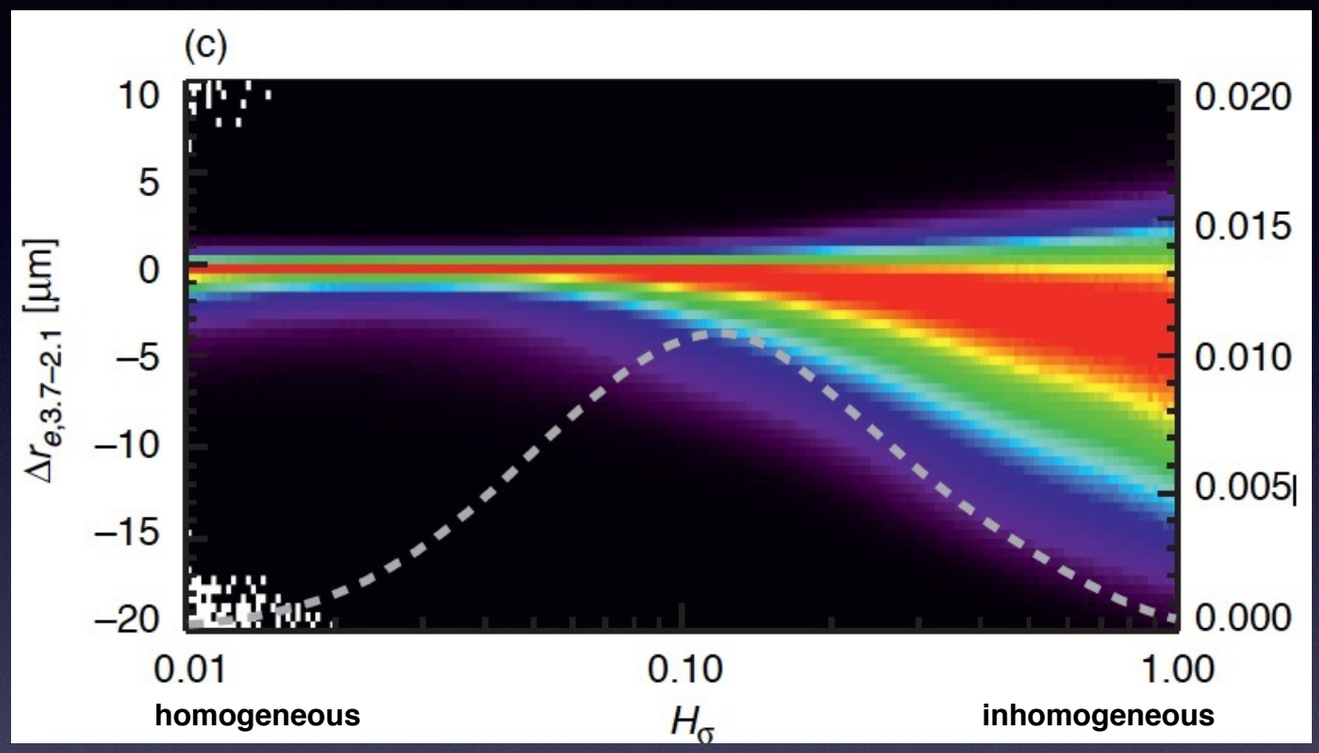

$$H_\sigma = \frac{std(R_{0.86}(250m))}{mean(R_{0.86}(250m))}$$

Liang et al. 2009

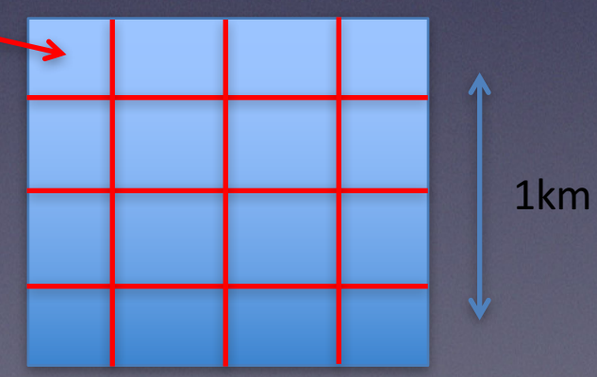

The difference between CER2.1 and CER3.7 (CER 3.7-CER2.1) increases when MBL cloud becomes more inhomogeneous. ~ PPHB or 3-D effects?

Independent pixel assumption?

LES cloud fields

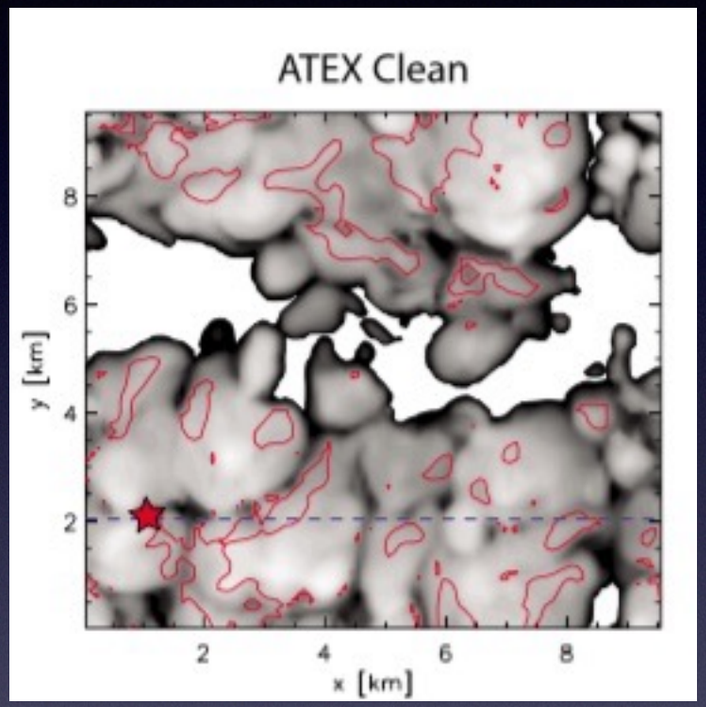

$$r_{e,\lambda} = r^{*}_{e,\lambda} + \Delta r^{3D}_{e,\lambda} + \Delta r^{PPHB}_{e,\lambda}$$

$$\left|\Delta r^{3D}_{e,2.1}\right| > \left|\Delta r^{3D}_{e,3.7}\right|$$

$$\Delta r^{PPHB}_{e,2.1} > \Delta r^{PPHB}_{e,3.7} > 0$$

Radiative Transfer Simulatons

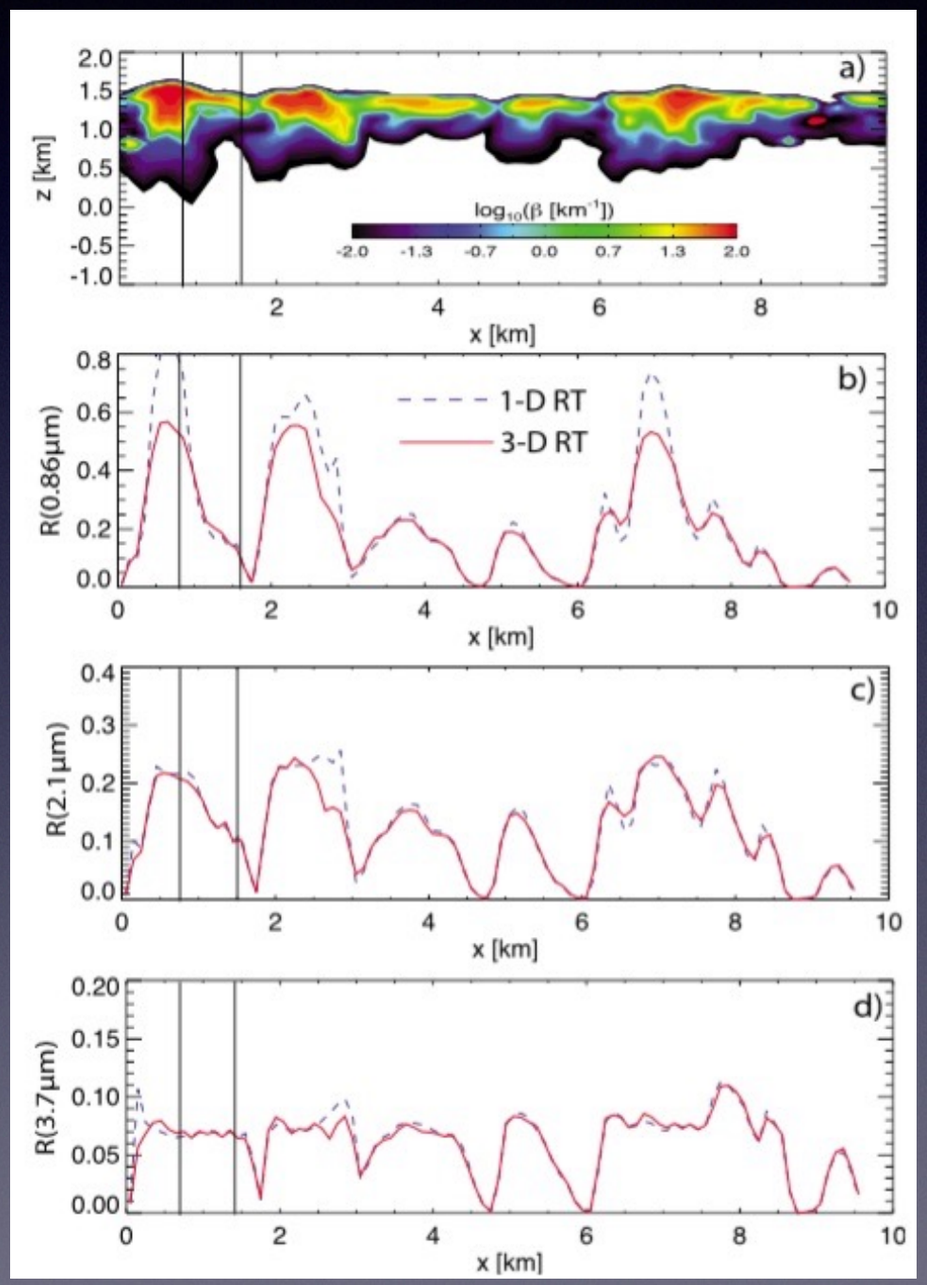

Zhang et al. 2012 JGR

Synthetic retrievals

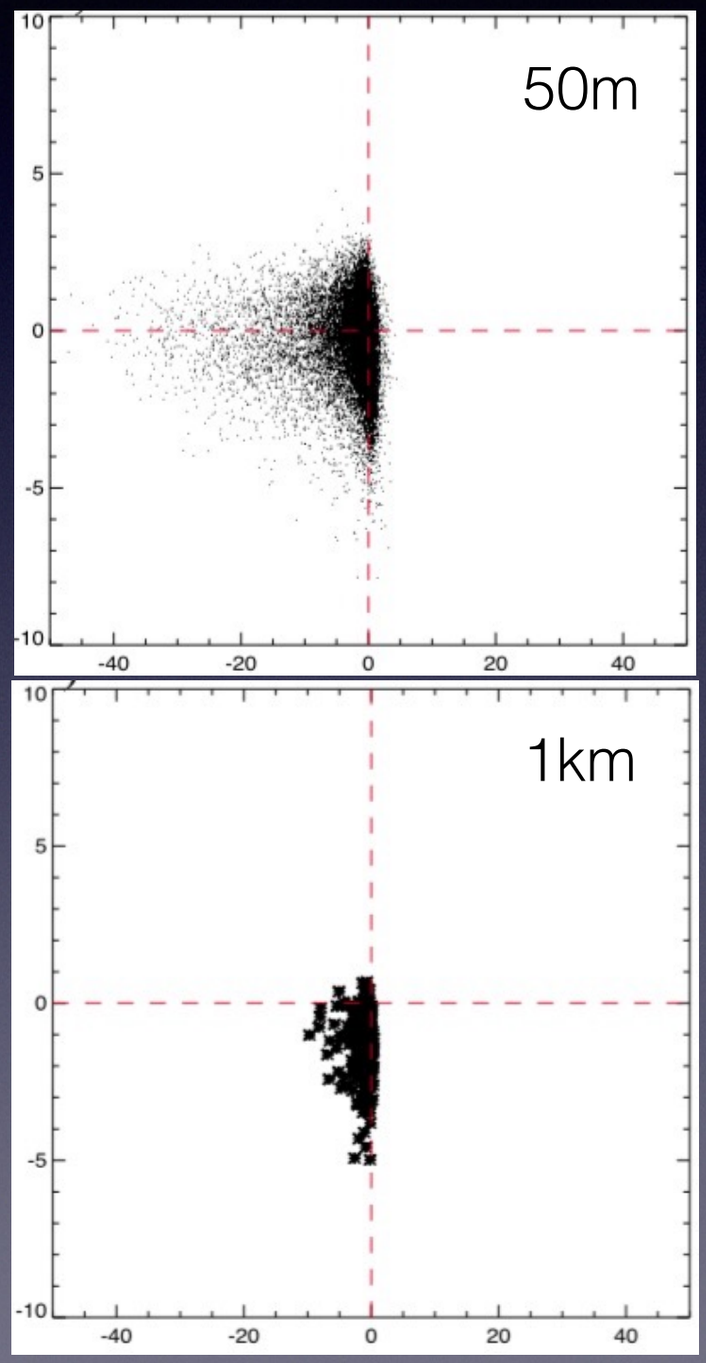

Other possible reasons

- Algorithm issues, e.g., bugs in the code, errors in ancillary data, etc.
- Cloud particle size distributions deviate from the assumed Gamma or Log-normal distributions [Zhang 2013 JQSRT].
- Surface contamination.
- Thermal correction in 3.7 μm retrievals.

Take-home messages

- Although looking at the same clouds, MODIS 3.7μm band retrieves significantly smaller CER for MBL clouds than the 2.1 μm band. This spectral CER difference has also been noted by other teams using independent algorithms.
- The difference shows a strong dependence on sub-pixel inhomogeneity (SPI), which cannot be explained by the “traditional” PPHB that assumes CER and COT retrievals to be independent.
- A new theoretical framework is developed to provide a more comprehensive understanding of how SPI influences both CER and COT retrievals in a mutually dependent way.
- The new framework can provide reasonable explanation for the spectral CER difference and its dependence on SPI.

Failed retrieval analysis

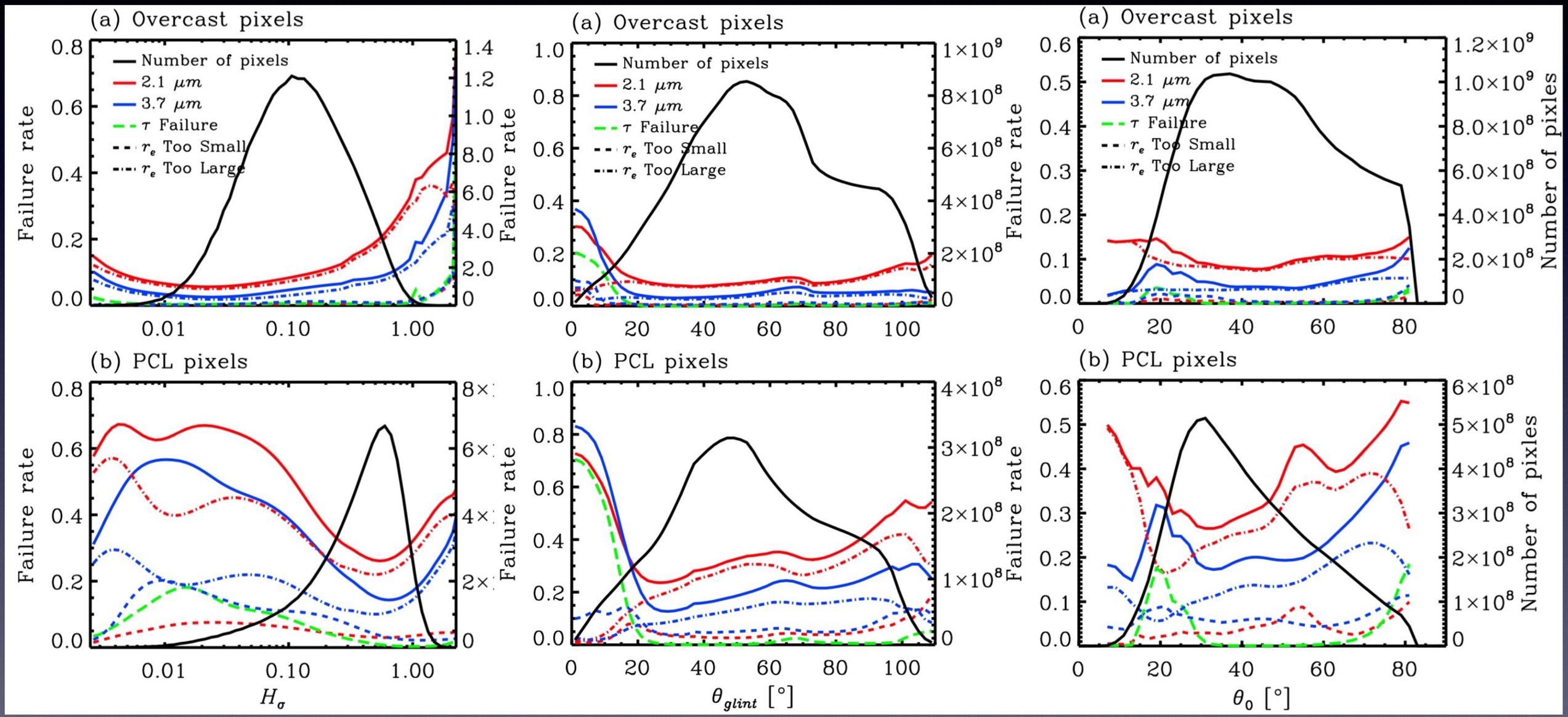

Failed retrieval analysis

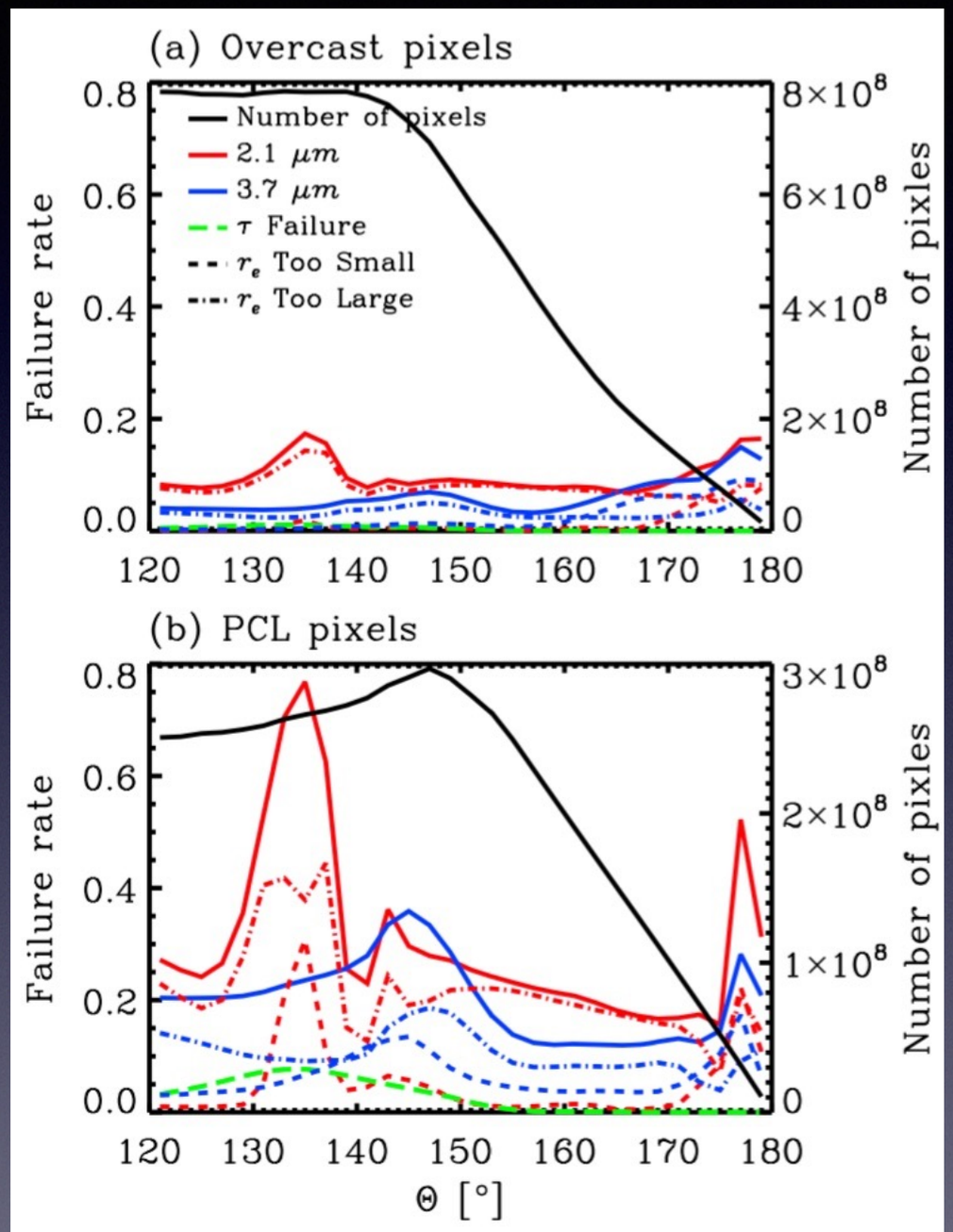

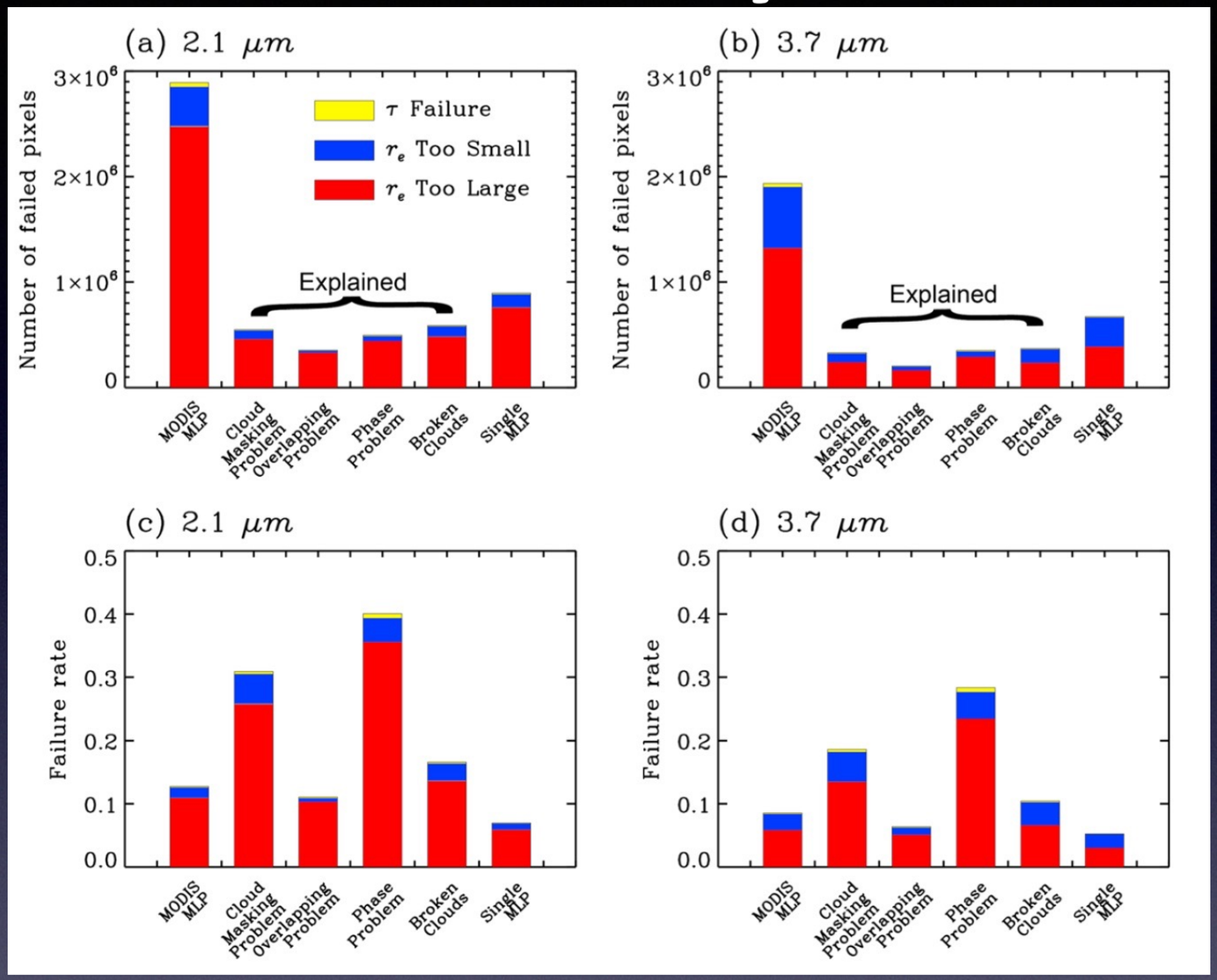

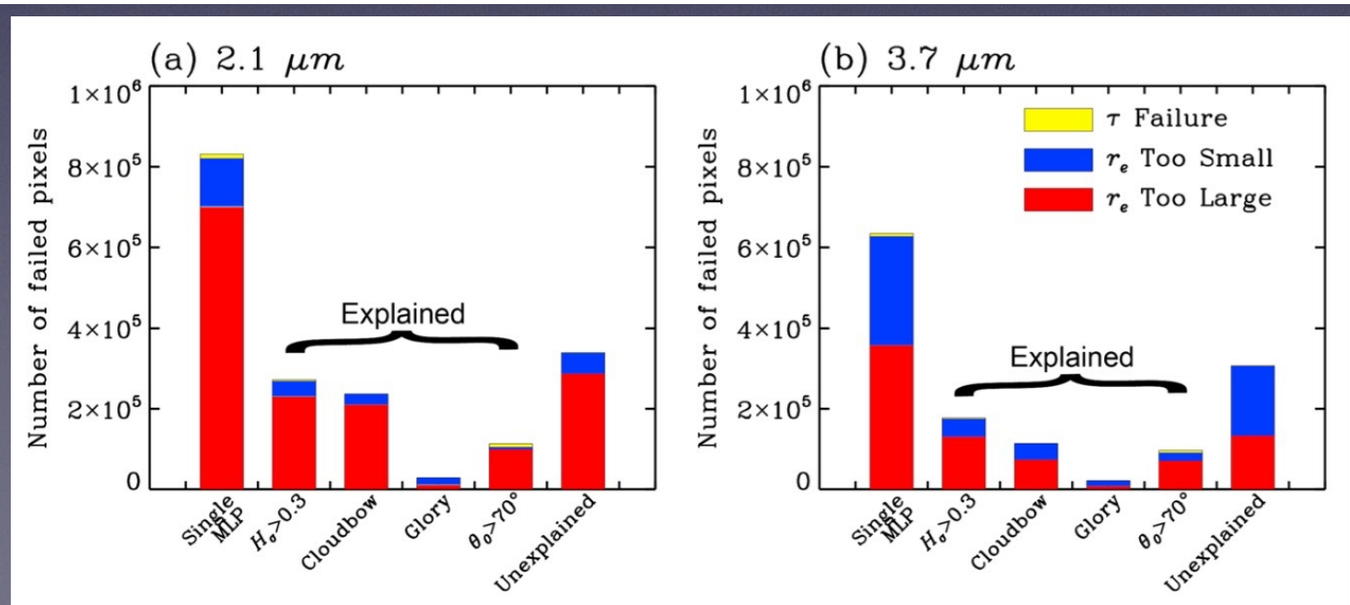

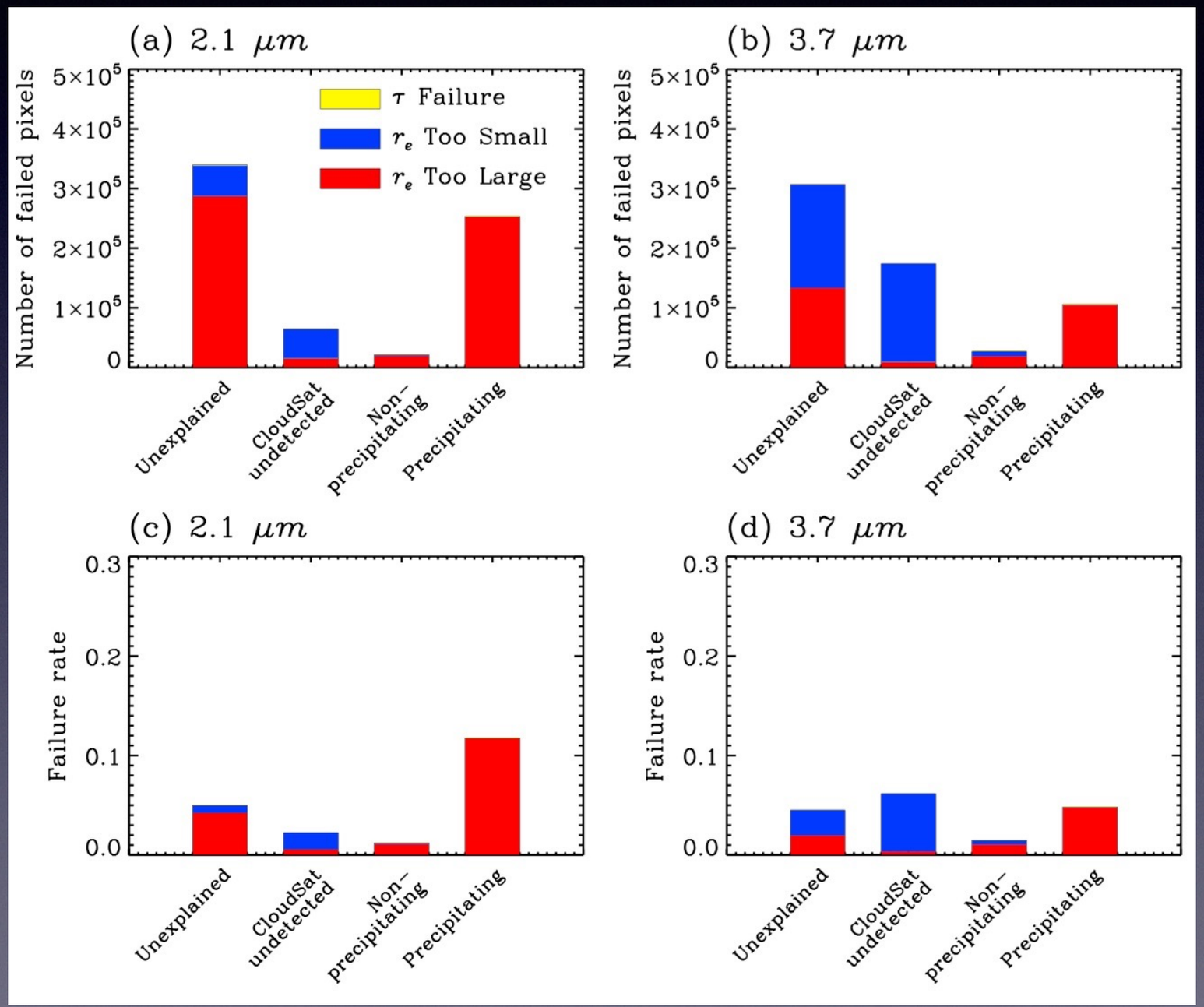
(a) 2.1 μm
(b) 3.7 μm
(c) 2.1 μm
(d) 3.7 μm
Number of failed pixels
Failure rate
τ Failure
r_e Too Small
r_e Too Large
5×10^5
4×10^5
3×10^5
2×10^5
1×10^5
0
0.3
0.2
0.1
0.0
Unexplained
CloudSat undetected
Non-precipitating
Precipitating